

Gonadogenesis in *Pristionchus pacificus* and organ evolution: development, adult morphology and cell–cell interactions in the hermaphrodite gonad

David Rudel^{*,1}, Metta Riebesell¹, Ralf J. Sommer

Max-Planck Institut für Entwicklungsbiologie, Abteilung Evolutionsbiologie, D-72076 Tübingen, Germany

Received for publication 25 June 2004, revised 14 September 2004, accepted 14 September 2004

Available online 7 October 2004

Abstract

The nematode gonad is an exemplary system for the study of organogenesis and fundamental problems in developmental and cellular biology. Nematode gonads vary dramatically across species (Chitwood, B.G., Chitwood, M.B., 1950. Introduction to Nematology. University Park Press, Baltimore; Felix, M.A., Sternberg, P.W., 1996. Symmetry breakage in the development of one-armed gonads in nematodes. Development 122, 2129–2142). As such, comparative developmental biology of gonadogenesis offers the potential to investigate changes in developmental and cellular processes that result in novel organ morphologies and thus may give insights into how these changes can affect animal baupläne. *Pristionchus pacificus* is a free-living nematode that diverged from the model nematode *Caenorhabditis elegans* around 200–300 million years ago. The morphology and development of *P. pacificus* is highly homologous to that of *C. elegans*. However, many differences in morphology and the underlying molecular signaling networks are easy to identify, making *P. pacificus* ideal for a comparative approach. Here, we report a detailed description of the *P. pacificus* hermaphrodite gonad using electron and fluorescent microscopy that will provide a basis for both phenotypic studies of genetic mutations and in vivo molecular studies of cloned genes involved in *P. pacificus* gonad development. We report that the morphology of the *P. pacificus* gonad is distinct from that of *C. elegans*. Among these differences are germ line patterning differences, heterochronic differences, novel gonadal arm-migrations, novel cellular composition of some somatic tissues (e.g., the number of cells that comprise the sheath and different spermathecal regions are different), the absence of a somatic tissue (e.g., the spermathecal valve cells), a novel architecture for the sheath, and changes in the cellular and sub-cellular morphology of the individual sheath cells. Additionally, we report a set of cell ablations in *P. pacificus* that indicate extensive cell communication between the somatic gonadal tissues and the germ line. Individual ablation experiments in *P. pacificus* show significant differences in the effects of individual somatic tissues on germ line patterning in comparison to *C. elegans*.

© 2004 Elsevier Inc. All rights reserved.

Keywords: *Pristionchus pacificus*; *Caenorhabditis elegans*; gonadogenesis; organogenesis; morphological novelties; heterochronic changes; evolution; morphology

Introduction

The nematode gonad has proven to be a cornucopia for the study of fundamental problems in cell biology and

developmental biology (Hubbard and Greenstein, 2000). The nematode gonad is a complex organ composed of both somatic and germ line tissues (for a review of adult *C. elegans* morphology, see the *Handbook of Worm Anatomy* on the Worm Atlas web site <http://www.wormatlas.org>). A diverse group of cellular processes are required during gonadogenesis and throughout the life of the adult animal. In the soma, the right number of cells for each tissue must be produced, they must arrange themselves into functional tissues, and they must interact appropriately with both the

* Corresponding author. Max-Planck Institut für Entwicklungsbiologie, Abteilung Evolutionsbiologie, Spemannstr. 37-39, D-72076 Tübingen, Germany. Fax: +49 7071 601 498.

E-mail address: david.rudel@tuebingen.mpg.de (D. Rudel).

¹ These authors contributed equally to this work.

germ line, for example, to regulate ovulation, and other nearby somatic tissues, for example, to initiate vulva formation. This requires regulated timing and positioning of cell divisions, cell migration, basal lamina remodeling, and complex intercellular signaling.

In the germ line, germ cells must be patterned in a specific manner. A germ line stem cell population must be maintained throughout the life of the animal; thus, the mitotic cell cycle must be highly regulated as well as the exit of mitosis and entry into meiosis. The nematodes discussed in this paper are hermaphroditic; thus, following entry into meiosis subsequent differentiation events must be properly triggered for individual germ cells, that is, development as a male gamete (a sperm), as a female gamete (an egg), or programmed cell death. Many of these germ line processes require crosstalk with the somatic gonadal tissues.

Given the plethora of processes that can be studied in the nematode gonad, the comparison of gonadogenesis among different nematode species is likely to provide a rich environment in which to study changes in cellular and molecular networks that have resulted in the biological novelties that help to make species distinct. This study is a description of the development of the gonad in the nematode *Pristionchus pacificus*. We compare what we find with what is known from *Caenorhabditis elegans* to identify differences in the morphology and cellular interactions between the gonads of these two species.

Decades worth of accumulated knowledge about the development of specific model organisms has led to the realization that all metazoans share a large common set of basic cellular and developmental processes and molecular players. However, the understanding of how the regulation of conserved cellular processes can change and how developmental cassettes are altered over evolutionary time-scales is in its infancy (Pires-DaSilva and Sommer, 2003). Additionally, from the sequencing of entire genomes, we now know that the genomes of even closely related species contain many novel putative genes, thus, the understanding of how novel molecular players and their functional interactions with conserved genetic networks arise is also in its infancy (Pires-DaSilva and Sommer, 2003). These questions require a comparative approach between related species. While we can often see differences in the molecular and cellular biology between model organisms, the evolutionary time that separates these systems are so large that interpreting differences is problematic. Detailed cellular and molecular genetic studies are required between species that are related enough that the body plans and the morphology of tissues can be recognized as homologous but far enough away that differences can be easily found (Rudel and Sommer, 2003; Simpson, 2002). Then, changes in the underlying developmental cassettes can be uncovered by experimental manipulation and by comparison of phenotypes and molecular networks among the related species.

Nematodes are ideal for a comparative evolutionary approach. First, there is a large collection of nematodes that are easily maintained in the laboratory. Second, these species have been arranged into a phylogenetic model that allows the placement and interpretation of differences between related species (Baldwin et al., 1997; Blaxter, 1998; Blaxter et al., 1998; Sudhaus and Fitch, 2001). Third, many fundamental genetic and molecular techniques that have been used originally in the model nematode *C. elegans* can be applied to these other nematode species (Sommer, 2000). Lastly, an immense body of developmental and molecular knowledge from *C. elegans* is available for comparison with data that can be accumulated from other nematode species.

In particular, the free-living nematode *P. pacificus* is ideal for comparative studies with *C. elegans*. *P. pacificus* diverged from *C. elegans* 200–300 mya (Pires-daSilva and Sommer, 2004) and the two worms share a highly homologous body plan. Detailed studies of vulva-formation, that is, formation of the organ through which embryos are expelled to the open environment, in *P. pacificus* demonstrate that many differences in cell interactions can be easily observed relative to *C. elegans* (Jungblut and Sommer, 2000; Sommer, 1997, 2001). In addition to its ideal phylogenetic position, *P. pacificus* is well developed for experimentation. An integrated physical and genetic map allow analysis of processes using forward genetics and *P. pacificus* has proven amenable to a variety of reverse genetic techniques (Pires-daSilva and Sommer, 2004). Most importantly for this study, *P. pacificus*, like *C. elegans*, has an invariant cell lineage and is transparent (Sommer and Sternberg, 1996b). Thus, *P. pacificus* is relatively easy to observe using standard Nomarski microscopy and individual cells can be identified and ablated using laser microbeam irradiation.

P. pacificus, like *C. elegans*, has two sexes; a hermaphroditic sex, essentially a self-fertile female that produces oocytes and some sperm, and a male sex that produces only sperm (Sommer et al., 1996). Like in *C. elegans*, male sperm is used preferentially upon mating. The gonads of these two sexes follow different developmental programs and have distinct adult tissue compositions and morphologies. The most obvious of these differences is the number of gonadal arms. The gonad of the hermaphrodite consists of two rotationally symmetrical reflexed tubes that encase the germ line and un-laid embryos. The two arms open into a common uterus at the anterior–posterior center of the animal (Fig. 1A). The uterus is connected to the outside via the vulva at the ventral midline. In contrast, the gonad of the male consists of a single reflexed arm that is attached to mating structures in the tail of the animal. Gonadal arms are patterned along their lengths, establishing a proximal–distal gonad specific axis. The description and the cell-ablation experiments in this manuscript focus on the *P. pacificus* hermaphrodite gonad.

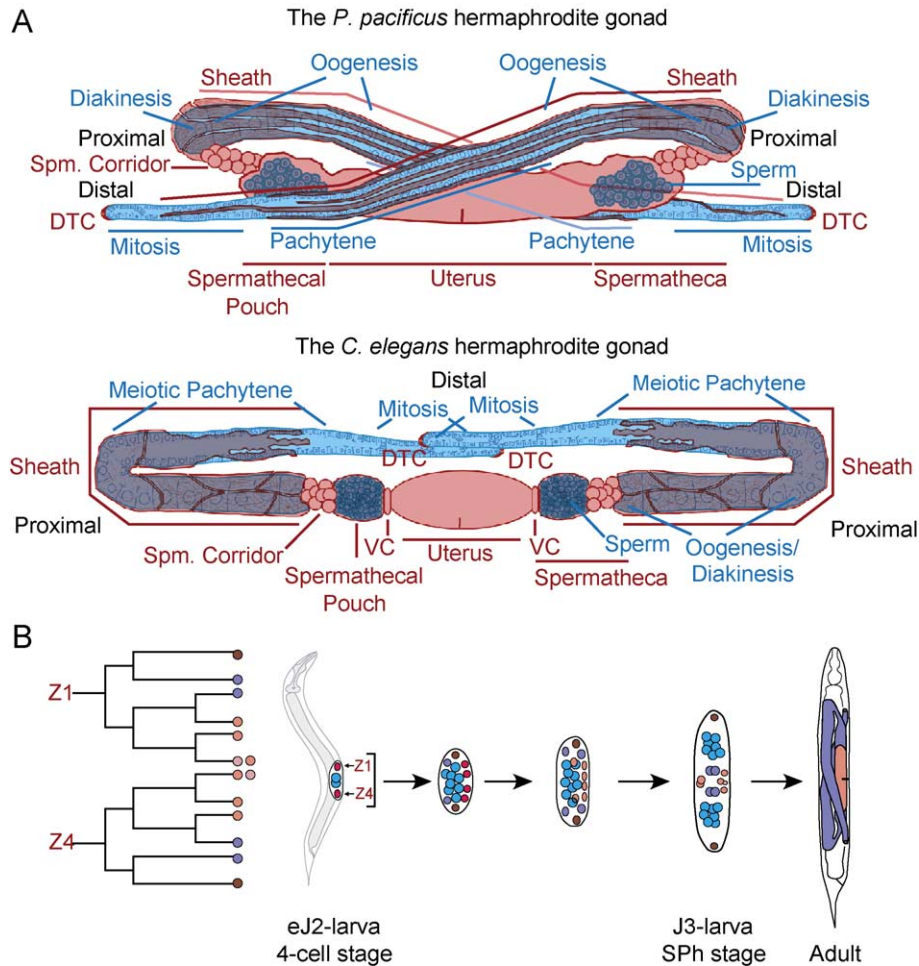


Fig. 1. An overview of the *P. pacificus* hermaphrodite gonad. (A) A cartoon comparison of the *P. pacificus* and *C. elegans* adult hermaphrodite gonads. Somatic tissues are shown in red. Germline tissues are shown in blue. Differences shown include: (1) The path of gonadal arm migration. (2) The morphology of the turn of the gonadal arms. (3) The cellular composition of the sheath and spermathecal corridor. (4) The cellular and sub-cellular morphology of the sheath (thin red lines represent actin filaments). (5) The absence of valve cells, VC, in *P. pacificus*. (6) The extent of diakinesis in the germ line. (7) A difference in size between sperm. (B) The development of the *P. pacificus* somatic gonad from the two somatic gonadal precursor cells Z1 and Z4. To the far left is a lineage diagram. Horizontal lines represent cells. Cell divisions are represented by branching. Divisions are shown to the SPh-stage. The predominate terminal fates are represented by color-coded circles: dark red, DTC. Purple, sheath/spermathecal precursor cells. Red, uterine cells. Pink, anchor cell. The anchor cell can develop from one of two precursor cells. To the right of the lineage diagram is a depiction of the gonadal primordium at various stages: 4-cell, the stage at which the DTCs are born, the stage in which all of the 12 somatic precursor cells are present, the SPh-stage when the somatic precursor cells rearrange to form a pre-pattern of the adult hermaphrodite gonad, and a representation of the adult gonad. Colored circles represent the position of nuclei within the developing gonad. Colors correlate with those in the lineage diagram. Blue circles represent germ cell nuclei.

Gonadogenesis in *P. pacificus* and *C. elegans* is punctuated by conserved developmental stages that are conceptually important (Felix et al., 1999). At these stages, specific cells are present that give rise to discrete tissues of the adult gonad. For *P. pacificus* hermaphrodite animals, these stages include the four-cell primordium present at hatching, the stage at which the distal tip cells (DTCs) are born, and the stage when all 12 founder cells are present and rearrange into a pre-pattern of the adult gonad (Fig. 1B). The last stage is termed the somatic gonadal primordium of the hermaphrodite, SPh. During the SPh-stage, many of the future somatic tissues are represented by an individual precursor cell or by subsets of these 12 precursor cells. These conserved developmen-

tal stages and precursor cells are the focus of the *P. pacificus* cell-ablation experiments discussed throughout this manuscript.

This is the first detailed description of gonadogenesis in a nematode other than *C. elegans*. We find that the gross morphology of the adult structures is quite different, the cellular composition (i.e., cell number) and morphology of individual tissue types have changed dramatically, and that differences can be observed in cell signaling between the somatic gonad and the germ line. Thus, the comparison of gonad development between *P. pacificus* and *C. elegans*, when complemented by genetic and molecular studies, can provide an important case study in evolutionary developmental biology.

Materials and methods

P. pacificus strains and maintenance

Animals were handled and *P. pacificus* strains were maintained as described for *C. elegans* (Brenner, 1974). With the exception of the ablation of the somatic gonad, that is, Z1 and Z4, *P. pacificus* (California) strain PS312 was used exclusively in this study (Sommer and Sternberg, 1996a). In the Z1 and Z4 cell ablation experiment, the *P. pacificus* (Washington) strain PS1843 was used in addition to strain PS312 (Srinivasan et al., 2001). All animals were maintained at 20°C.

Developmental staging and timing of larvae and adults

To stage animals, 50 adult hermaphrodites from a mixed stage culture were transferred to a fresh agar plate seeded with *Escherichia coli* strain OP50. Animals were allowed to lay eggs for approximately an hour and then removed. *P. pacificus* hermaphrodites do not retain eggs in the uterus and eggs are laid at the one to four-cell stage. Eggs were grown at 20°C and developing larvae observed by microscopy for staged experiments.

Fluorescent staining of gonadal arms

Dissection of gonadal arms was accomplished as follows: staged animals were transferred by mouth-pipette into a drop of PBS with 0.25 mM levamisole contained within an etched ring on a microscope slide. Under a dissecting microscope and using a 27-gauge disposable hypodermic needle, animals were decapitated at the base of the pharynx. Upon decapitation, the body muscle contractions squeezed the gonadal arms to the outside of the carcass.

To fix the tissues, either intact worms or dissected gonadal arms with their associated carcasses were transferred by mouth pipette into the well of a depression slide containing a solution of 2% paraformaldehyde (PFA) in PBS. Worms and gonads were allowed to fix in the solution for 1 h on ice. The PFA solution was removed and the gonads were washed in a fresh PBS solution for 15 min on ice. Then, samples were extracted using one of two methods. Extraction 1: the PBS was removed and the sample was extracted sequentially with methanol (–20°C) for 5 min and with acetone (–20°C) for 5 min. After removal of the acetone, the sample was re-hydrated in PBS for 15 min. The old PBS was then replaced with a fresh PBS solution containing the dye of interest. Extraction 2: the PBS was removed and the sample was extracted with a 0.1% Tween-20, 0.5% BSA egg salts solution for 10 min. The detergent solution was removed and the sample washed in fresh egg salts solution. The wash was then replaced with fresh egg salts solution containing the dye of interest. To stain actin filaments fluorescently labelled phalloidin was used at a final concentration of approximately 0.15 µM

(AlexaFluor® 488 Phalloidin A-12379 or AlexaFluor® 546 Phalloidin A-22283, Molecular Probes). To stain DNA 4',6-diamidino-2-phenylindole, DAPI, was used at a final concentration of 1 µg/ml (D-1306, Molecular Probes). Worms and gonads were stained for 30 min to 6 h.

Fixed worms and dissected gonads were mounted in a drop of VectaShield mounting medium (H-1000, Vector Laboratories, Inc.) on a 5% agar in water pad. Samples were viewed on an Axioplan 2 microscope (Zeiss) using a Polychromator Illumination System (Visitron Systems, GmbH). Pictures were taken using the Meta View program (version Meta Series 4.5, Visitron Systems, GmbH) and a digital camera (MicroMax 5MHz System, Princeton Instruments, Inc.).

Cell ablations

Cell ablation experiments were carried out using standard techniques described for *C. elegans* (Epstein and Shakes, 1995) using a MicroPoint Ablation Laser System from Laser Science, Inc. For mounting, animals were transferred by mouth pipette to a drop of PBS on a pad of 5% agar in water containing 10 mM sodium azide as an anaesthetic. All ablation experiments were repeated as independent sets of ablations at least twice.

Scanning electron microscopy

SEM preparation of isolated gonadal arms of *P. pacificus* was carried out using previously described techniques (Hall et al., 1999). Young adult hermaphrodites were decapitated in a small glass Petri dish in 1× PBS containing 0.05% Tricaine/0.005% Tetramisole. The extruded gonads were separated from their carcasses and transferred to flow-through micro-chambers floating on 1× PBS (Hausen and Riebesell, 2002). Dish, needles and capillary of mouth-pipette were BSA-coated to avoid sticking. To remove the gonadal basal lamina, the gonads were treated with 0.1 mg/ml collagenase (type II, Sigma C-6885) in PBS for 20 to 50 min. After digestion, the gonads were put on ice, washed in cold PBS, fixed in 3% glutaraldehyde in 0.1 M sodium phosphate buffer (pH 7.0) for 2 to 12 h and washed three times for 15 min each in cold 0.1 M sodium phosphate buffer (pH 7.0) containing 5% sucrose. After that they were postfixed in 1% osmium tetroxide in PBS for 1 h followed by washing in PBS. Gonads were removed from the flow-through chambers and transferred to small PBS-filled specimen capsules (Sigma C-1178) to avoid damage during dehydration. The capsules were passed through a series of graded ethanols followed by critical point drying with carbon dioxide. The dried gonads were taken out of the capsules using an insect needle with a sticky tip (glue scratched off a double stick tape) and mounted on aluminum stubs covered with double stick tape. The specimens were sputter-coated with gold. A Hitachi S-800 Scanning Electron Microscope was used for inspection.

Transmission electron microscopy

Living worms were cryoimmobilized by high-pressure freezing. In short, young adult hermaphrodites were put into 100 mm deep aluminum platelets half filled with a thick *E. coli* paste (OP50 either scratched off a bacterial lawn or spun-down from a liquid culture). A small drop of 50 mM sodium azide in M9 was added to the worms that were intended for longitudinal sectioning, the platelet was then filled up with 1-hexadecene. J2 larvae were added to an *E. coli* suspension and sucked into cellulose capillaries (Hohenberg et al., 1994). Two-millimeter-long capillary tube segments were transferred to aluminum platelets of 200 μm depth containing 1-hexadecene. The platelets were sandwiched with aluminum platelets without any cavity and then frozen with a high-pressure freezer (Bal-Tec HPM 010, Balzers, Liechtenstein). The frozen worms and capillary tubes were freed from extraneous hexadecene under liquid nitrogen and transferred to 2 ml microtubes with screw caps (Sarstedt #72.694) containing the substitution medium pre-cooled to -90°C . Samples were kept in 2% osmium tetroxide in anhydrous acetone at -90°C for 32 h, at -60°C for 4 h, and at -40°C for 7 h in a freeze-substitution unit (Balzers FSU 010, Bal-Tec, Balzers, Liechtenstein). After washing with acetone the samples were infiltrated with Epon and polymerized at 60°C for 48 h. Ultra-thin sections were stained with 2% uranyl acetate in 50% ethanol for 30 min and 0.4% Pb citrate for 3 min. Sections were viewed in a Philips CM10 electron microscope at 60 kV.

Statistical analysis

Averages and standard errors were computed using Microsoft Excel for the Mac. Standard error was computed by dividing the sample standard deviation by the square root of the sample size.

Results and discussion

P. pacificus development occurs during larval stages. During each larval stage, discrete well-conserved developmental events take place. These larval stages therefore provide a convenient time line for the description of developmental processes in nematodes. Previously, the presence of three post-hatching larval stages, named J1–J3, was reported in *P. pacificus* (Felix et al., 1999). Recent studies indicate the existence of a fourth pre-hatching larval stage, determined by a pre-hatching molt within the eggshell (Sudhaus and Fürst von Lieven, 2003). We will from now on refer to the pre-hatching larval stage as J1 and the post-hatching larval stages as J2–J4. In comparison, *C. elegans* has four post-hatching larval stages, L1–L4, and no pre-hatching molts. We view the four larval stages of *P. pacificus* and *C. elegans* to be homologous. The develop-

ment of the *P. pacificus* gonad is highly regulated and precisely reproduced among all animals. However, the morphology of individual gonad developmental stages and the timing of gonad developmental events with respect to the four cuticle molts are divergent with respect to that of *C. elegans*.

Early development of the *P. pacificus* gonad

The 4-cell gonadal primordium has a novel geometry in *P. pacificus* in comparison to that of *C. elegans*. At hatching, the gonad of the early *P. pacificus* J2-larvae is present as a primordium of four cells surrounded by a basal lamina. The 4-cell primordium is located along the ventral side of the animal at the anterior–posterior center of the body (Figs. 1B, 2A). Two cells are found on the right side of the animal, Z1 and Z2, and two cells are found on the left side of the animal, Z3 and Z4. The cells on the right side of the animal are anterior to those on the left side. The outer cells, Z1 and Z4, give rise to the somatic gonadal tissues (Fig. 1B); the inner cells, Z2 and Z3, are the progenitors of the germ line. Z2 and Z3 overlap along the anterior–posterior axis (Figs. 2C, E). Tracings of sequential horizontal TEM sections indicate that in *P. pacificus* each of the four founder cells can contact the other founder cells. This is due to extensions of Z1 and Z4 that meet at the midline to cup Z2 and Z3 along the ventral side of the primordium. These extensions invaginate extensively between Z2 and Z3 (Fig. 2E), though Z2 and Z3 do contact each other (Fig. 2C). In *C. elegans*, during the L1 stage, the four homologous gonadal founder cells lie in a row along the ventral midline at an angle with respect to the right–left axis (Fig. 2B). Often three of the cells, but occasionally all four, may be found in a lateral focal plane (Kimble, 1981; Kimble and Hirsh, 1979). The nuclei of the two primordial germ cells never overlap along the anterior–posterior axis as in *P. pacificus*. The somatic precursor cells Z1 and Z4 cup the primordial germ cells and make contact with each other on the ventral side of the four-cell primordium (Mathies et al., 2003; Siegfried and Kimble, 2002). It has been hypothesized that this contact may play a role in establishing an early gonad polarity in the somatic cells in *C. elegans*, via signaling through a *Wnt* pathway (Siegfried and Kimble, 2002; Siegfried et al., 2004). As these contacts are present within the *P. pacificus* gonad four-cell primordium despite its unique morphology, they may play a similar role in establishing a *P. pacificus* gonadal asymmetry.

A pre-pattern for the adult gonad is established during the J2 and J3 stage in *P. pacificus* homologous to that of *C. elegans* (Felix et al., 1999). During the late J2 stage, the somatic gonadal precursor cells divide to produce the 12 founder cells that give rise to all the adult somatic structures (Fig. 1B). During the early J3-larval stage, 10 of these founder cells coalesce at the centre of the developing gonad into a symmetrical blue print for the adult gonad; this stage is known as the somatic primordium of the hermaphrodite,

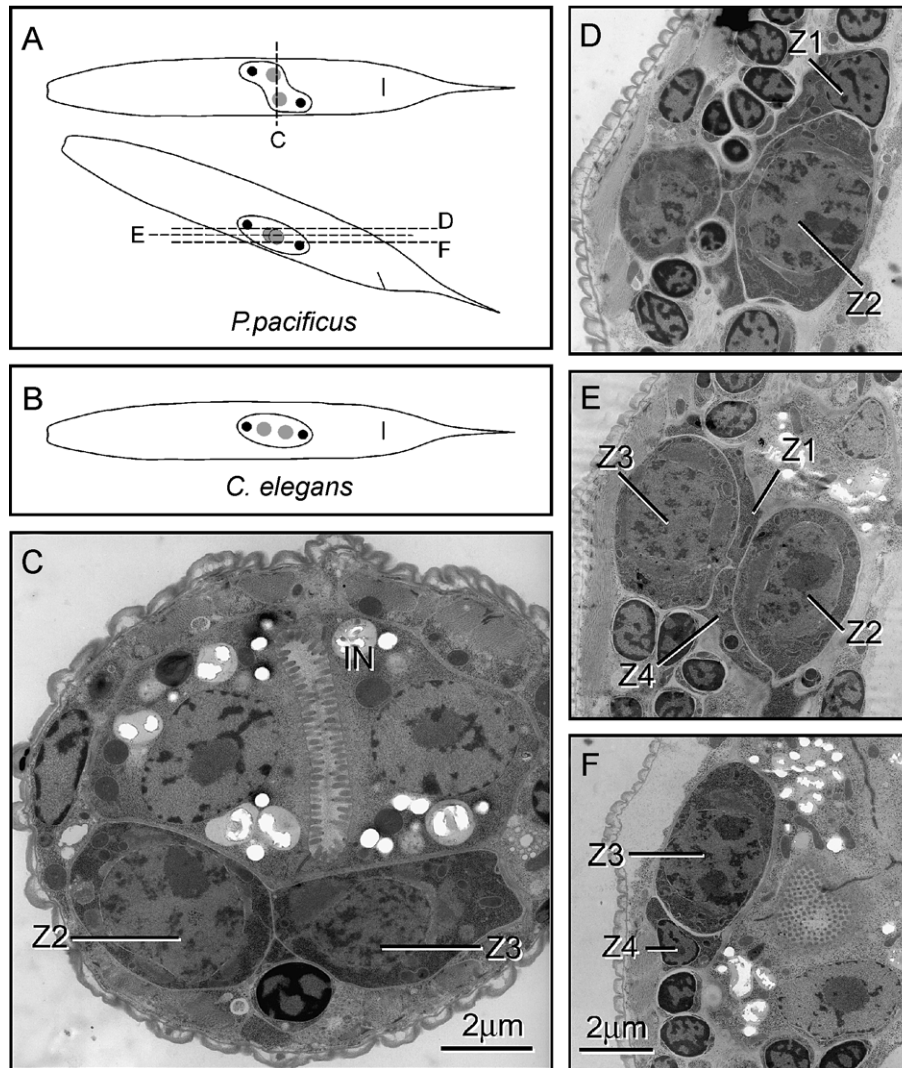


Fig. 2. The geometry of the 4-cell gonadal primordium. (A) The top cartoon is a dorsal view of a *P. pacificus* larva at J2 stage after hatching. The bottom cartoon is a lateral view. The 4-cell gonadal primordium is shown. The anus is represented by a slit in the posterior. The nuclei of the somatic precursors Z1 and Z4 are represented as solid black ovals, the nuclei of the germ line precursors Z2 and Z3 as grey circles. Precursor cells are numbered from anterior to posterior. Dashed lines represent the relative placement of TEM sections shown in the subsequent panels. (B) A depiction of a dorsal view of the *C. elegans* L1 stage after hatching showing the 4-cell gonadal primordium. Precursor cells are represented as in panel A. (C) A transverse TEM section through a J2 stage animal. The intestine, IN, and the gonadal precursor cells are labeled. (D–F) Sequential horizontal TEM sections through a J2 stage animal. The gonadal precursor cells are labeled.

SPh (Fig. 1B). The remaining two founder cells become the DTCs. In the process of SPh formation, the somatic gonadal cells subdivide the mitotically dividing germ cells into an anterior and a posterior population. Each of these 10 founder cells subsequently undergoes a discrete set of species-specific reproducible divisions to produce the cells that comprise the adult tissues. During the J3 stage, the two ovotestis also begin to elongate along the ventral body wall (Fig. 3), one anteriorly and one posteriorly, each led by a DTC.

Gonadal arm migration in *P. pacificus*

The path of arm migration for the *P. pacificus* hermaphrodite gonad during development is novel in comparison to

that of *C. elegans* and results in a dramatic change in the gross morphology of the gonad (Figs. 1A, 3). Following an initial elongation along the ventral body wall, the gonadal arms in *P. pacificus* migrate dorsally in the early J4 stage (Fig. 3). Upon reaching the dorsal side of the animal, the gonadal arms migrate back towards the center of the animal and meet above the vulva in the late J4 stage. At the time of the J4/adult molt in *P. pacificus*, the arms of the hermaphrodite gonad make a ventral migration and return to the ventral side of the body. There, lastly, upon reaching the body wall they continue to migrate along the ventral side of the animal, one to the anterior and one to the posterior of the animal (see the left side of Fig. 3). This results in a sort of squashed pretzel-like shape for the *P. pacificus* gonad in vivo. The elongating gonad is encased in a basement

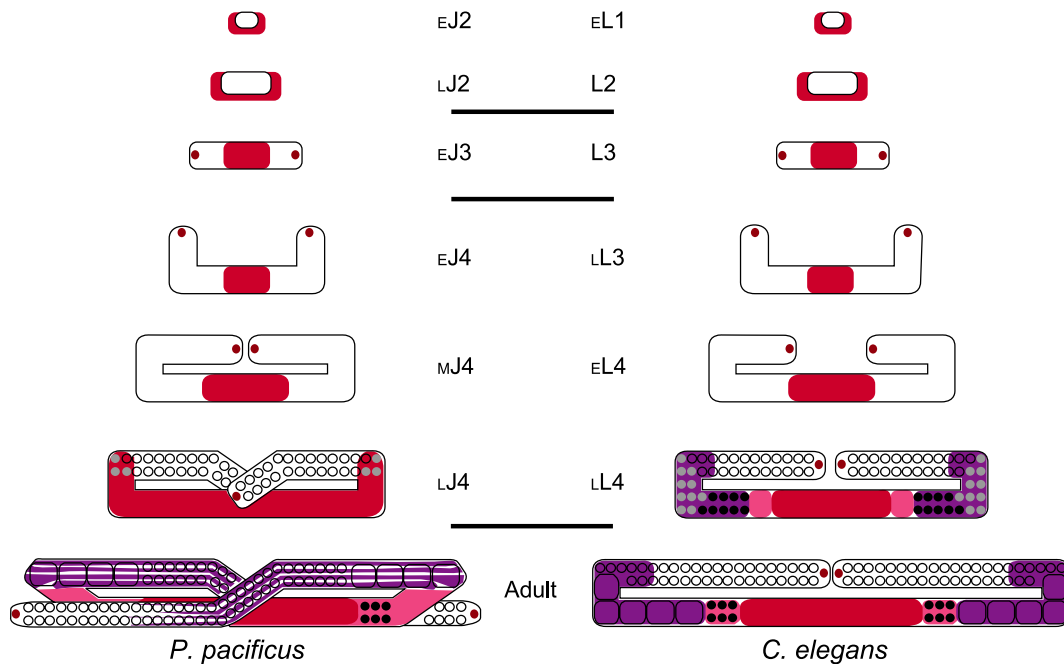


Fig. 3. The developmental timing of hermaphrodite gonadogenesis in *P. pacificus* and *C. elegans*. To the left, developmental gonad stages correlated with larval stages in *P. pacificus*. To the right, developmental gonad stages correlated with larval stages in *C. elegans*. Small caps E, M, and L denote early, mid, and late larval stages respectively. Germ line tissues are shown only from LL4 to adult. Mitotic and meiotic germ cell nuclei are represented as open circles. Spermatocyte nuclei are represented as solid grey circles. Sperm nuclei are represented as solid black circles. Oocytes are represented as open rounded blocks. Somatic structures are color-coded: Developing tissues, light red. Uterus (In adult stages and LL4 *C. elegans* larvae), red. DTCs, dark red. Sheath, purple. Spermatheca, pink.

membrane that contributes to the maintenance of its overall morphology and integrity. As the gonadal arms extend this basal gonadal lamina must be continuously remodeled and expanded. The arms of the *C. elegans* hermaphrodite gonad make a similar set of migrations (Fig. 3, right side). However, the *C. elegans* arms migrate further along the ventral body wall before turning dorsally and the arms never make a ventral migration to return to the ventral body wall (Hirsh et al., 1976; Kimble and White, 1981). This results in two U-shaped gonadal arms. Thus, early gonadal migrations in *P. pacificus* and *C. elegans* are similar, but later migrations differ and result in disparate adult gross gonadal architectures.

The timing of gonadal tissue differentiation

The somatic gonadal tissues have a specific temporal order of differentiation. Throughout the J2 and J3-stage, while the somatic gonad is developing into the SPh-stage primordium, the progeny of the germ line precursor cells appear to divide in a random fashion. With the formation of the SPh, however, the germ cells become divided into two populations and are subsequently patterned along the distal–proximal axis in a life cycle dependent fashion (Fig. 3). At the mid J4-stage, the somatic founder cells have divided to produce most or all of the precursor cells of the adult somatic tissues. The somatic cells are arranged in two aligned rows that form the proximal part of the gonadal arm, which lies along the ventral side of the animal. All germ

cells have been excluded and pushed beyond the bend into the distal part of the gonadal arm, which lies along the dorsal side of the animal (Fig. 3). Based upon nuclear morphology, the most distal four pairs of somatic cells are the first to show signs of differentiation. These are the future sheath cells which will cap the proximal germ line. Subsequently, the next five pairs of cells proximally, the presumptive spermathecal corridor cells, show signs of differentiation, that is, their nuclei become smaller. Concurrently, the sheath cells begin to change their cellular morphology; they start to express actin in filaments and to extend processes. The cells of the spermatheca and uterus remain difficult to distinguish from each other by DAPI staining and morphologically by Nomarski microscopy into the J4/adult molt. Full differentiation of all somatic tissues is completed only in the adult (Fig. 3, LJ4 and Adult). In *C. elegans*, somatic gonadal tissues are highly differentiated by the late L4-stage and already exhibit an adult morphology (Fig. 3, LL4 and Adult) (Kimble, 1981; Kimble and White, 1981).

Concurrent with the delay in differentiation of somatic structures, the differentiation of gametes is delayed with respect to the last molt in *P. pacificus* in comparison to *C. elegans* as well. At early J4-stage, only the distal germ cells are undergoing mitosis, a transition zone from mitosis to meiosis has already been established and the most proximal germ cells are in pachytene. The first gametes produced are sperm. Primary spermatocytes are first observable as animals approach the J4/adult molt (Fig. 3, LJ4). Spermatogenesis

continues into adulthood and the first sperm are produced shortly after the last molt. Subsequently, spermatogenesis is switched off and the first oocytes are produced 4 to 6 h following the molt (Fig. 3, Adult). The maturation and ovulation of the first oocyte in adulthood is required to push the sperm into the spermatheca in *P. pacificus*. Ten to 12 h following the last molt, young *P. pacificus* adult hermaphrodites begin to lay eggs (approximately 56–60 h after hatching at 20°C). Most *P. pacificus* eggs are laid at the two- to four-cell stage. By comparison, in *C. elegans*, primary spermatocytes are present in the mid- to late-L4 stage and some sperm are already produced by the L4/adult molt (Fig. 3); during the first hour or two of early adulthood, spermatogenesis is turned off and the first oocytes are produced. Twelve to 14 h following the last molt, *C. elegans* adult hermaphrodites begin to lay eggs (approximately 58–62 h after hatching at 20°C). In contrast to *P. pacificus*, *C. elegans* hermaphrodites usually retain several eggs in the uterus.

Taken together, comparison of the timing of gamete and somatic gonad differentiation with respect to the timing of the molt into adulthood in both *P. pacificus* and *C. elegans* reveals a major heterochrony of post embryogenesis. The involvement of heterochronic changes in developmental programs as a principal factor effecting major changes in metazoan bauplän throughout evolution is a central topic in discussions of ontogeny and phylogeny (Gould, 1977; McKinney, 1988). In particular, the importance of constraints placed upon ontogeny by heterochronic changes in the differentiation of the germ line and the reproductive system at large has been promoted (Gould, 1977). Changes in the regulation of the timing of major morphogenetic events in the nematode gonad relative to larval stages and other developmental programs offer inroads into exploring these issues in an experimental context. The corresponding shifts in germ line differentiation and somatic tissue differentiation in *P. pacificus* in comparison to *C. elegans* is a case in point. It seems that either the shift in the timing of gamete differentiation allowed a shift in the timing of differentiation of the somatic structures or that the shift in the timing of somatic tissue differentiation in *P. pacificus* required a concurrent shift in the timing of gamete differentiation. As germ line patterning is highly dependent upon the somatic gonad (explained later in the text) the latter seems more likely.

The germ line of P. pacificus

The position of the germ line in vivo is novel in *P. pacificus*. First, except for the sperm stored in the spermatheca and fertilized eggs, in adult *P. pacificus* animals, the proximal germ line lies in its entirety along the dorsal side of the animal. A sharp elbow forms the bend of the *P. pacificus* gonadal arm. This constrains the germ line to the dorsal side of the animal (Fig. 1A). During fertilization and ovulation, oocytes are squeezed ventrally into the spermatheca proper through a tight opening in the

sheath and the spermathecal corridor. Second, due to the unique ventral migration of the *P. pacificus* hermaphrodite gonadal arms, the distal mitotic zone of each gonadal arm lies along the ventral side of the animal. In contrast, the bend of the gonadal arm is a smooth U-turn in *C. elegans*, thus developing oocytes extend around the bend into the proximal ventral region of the arm (Hirsh et al., 1976; Kimble and White, 1981). Also, as there is no ventral migration in *C. elegans*, the distal gonadal arm remains hugged against the dorsal body wall. Thus, the final morphology and composition of the individual tissues are quite different in *P. pacificus* in comparison to *C. elegans* (Fig. 1A).

The *P. pacificus* germ line can be divided into regions based upon the state of the DNA in the nuclei visualized by DAPI in situ staining of dissected adult hermaphrodite gonadal arms (Fig. 4A): a mitotic zone (MZ) where approximately 19 nuclei (18.87 ± 0.26) can be counted in a line along the proximal–distal axis, a transition zone (TZ) between mitosis and meiosis of approximately 6 nuclei (5.87 ± 0.22) as determined by the nuclei's characteristic crescent shape, a pachytene zone (PZ) of approximately 23 nuclei (22.65 ± 0.46) characterized by nuclei with condensed chromatin strands, and in adults a growth zone (GZ) of approximately 8 nuclei (7.56 ± 0.28) where gametes differentiate, that is, these germ cells enlarge and the nuclei leave pachytene and enter diakinesis, numbers in parentheses are the sample averages for 23 gonad arms and the associated standard errors. The numbers given are for staged adult animals that have been laying embryos for 24 h. Occasional cell deaths may be observed throughout the pachytene region and at the start of the growth zone. In very young adults spermatocytes are differentiated in the region later taken up by the growth zone. Transition from spermatogenesis to oogenesis is stark. While similarities exist (Crittenden et al., 1994; Hirsh et al., 1976; Kadyk and Kimble, 1998; Kimble and White, 1981), the patterning of the germ line in *P. pacificus* exhibits differences in comparison to *C. elegans*. First, the length of the transition zone is reduced in comparison to that of *C. elegans*, where it is 10 nuclei in length. Second, in *P. pacificus*, there is on average a single oocyte in each arm in diakinesis at any given time (0.82 ± 0.14), whereas in *C. elegans*, several late stage oocytes within an arm are in diakinesis. Third, the sperm of *P. pacificus* are significantly larger than the sperm of *C. elegans*, 9.3 μm in diameter for *P. pacificus* unactivated sperm versus 5.9 μm in diameter for *C. elegans*. *C. elegans* hermaphrodites also exhibit a stark switch from spermatogenesis to oogenesis.

The germ line of *P. pacificus* is syncytial (Fig. 4B). TEM of transverse and longitudinal sections through the gonad confirms that individual germ cells that reside at the periphery of the arm are open to a common cytoplasmic core in the center, called the rachis (Fig. 5B). Additionally, in situ staining of actin using phalloidin to determine germ cell borders indicates that every germ cell nucleus is

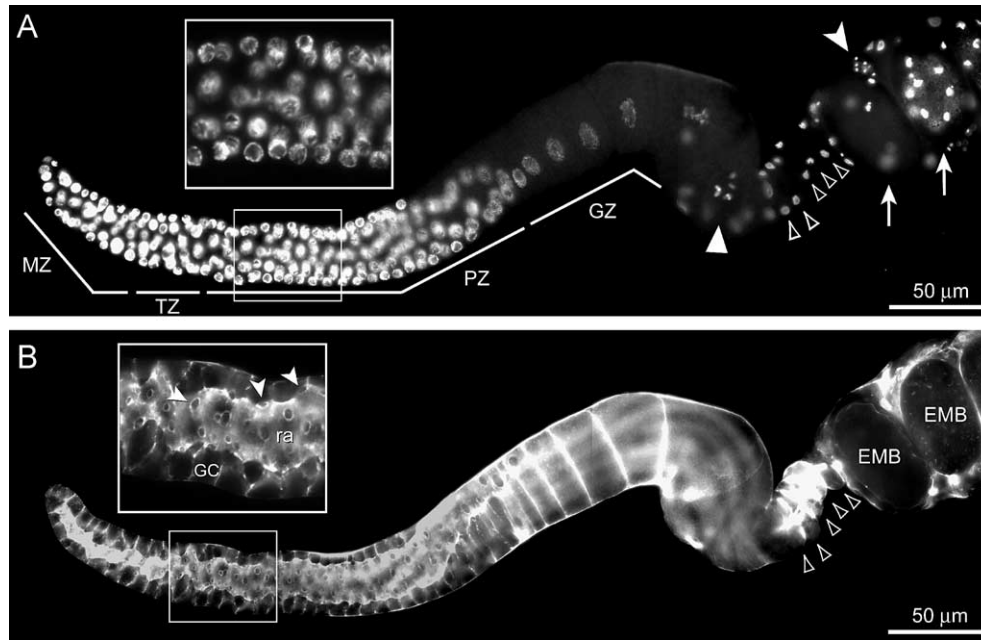


Fig. 4. The *P. pacificus* germ line is patterned along the proximal–distal axis and is syncytial. Panels A and B show a dorsal view of the same dissected gonadal arm at the same focal plane, approximately midway through the arm. Distal is to the left. This arm is the same arm shown in Fig. 6. This arm is from a young adult; as such, the extent of the individual regions in terms of the number of nuclei in a line along the distal–proximal axis is slightly smaller than that given for staged animals in the text. (A) Dapi staining reveals the morphology of nuclei. Germ line regions are indicated and labeled: Mitotic zone, MZ. Transition zone, TZ. Pachytene zone, PZ. Growth zone, GZ. The oldest oocyte is in diakinesis with diplotene chromosomes, large triangle. Sperm are highly condensed small foci, arrowhead. Two arrows mark the position of embryos. Five open tapered arrowheads mark the position of paired spermathecal corridor cell nuclei. The insert is a blowup of the region indicated by the small box below and shows nuclei that are in pachytene. Visible highly condensed strands of DNA characterize pachytene nuclei. (B) Phalloidin stains the actin lining cell membranes. Distally, the small transverse lines along the periphery of the germ line are germ cell borders. Proximally, the large transverse lines are the borders between maturing oocytes. The brightly staining cells proximal to the germ line are the five pairs of spermathecal corridor cells, marked by open tapered arrowheads. Spermathecal corridor cells contain large amounts of cytoplasmic filamentous actin. Embryos, EMB, are labeled. The brightly staining core of the distal germ line is the surface of the rachis, a communal cytoplasm shared by all the cells of the germ line. Germ cells are only partially encased by membrane and are open to the rachis by large circular “manhole-like” gaps. The insert is a blowup of the region indicated by the small box below. Arrowheads mark individual openings from germ cells into the rachis.

surrounded by an incomplete cell membrane that opens to the rachis by a single round passage (Fig. 4B insert). The germ line of *C. elegans* is also syncytial and the germ cells are arranged around the periphery of the arm and open into a common cytoplasmic core. However, the germ cells of *P. pacificus* are slightly larger than the germ cells of *C. elegans*. The syncytial nature of the *P. pacificus* germ line makes it potentially straightforward to introduce molecules, such as morpholino oligo nucleotides, dsRNA, or DNA constructs, into gametes and future progeny by direct injection into the rachis of the germ line.

Development of the P. pacificus somatic gonad does not require the germ line

The germ line is not required for the development of the somatic gonad in *P. pacificus*. The development of the germ line and the somatic gonad is concurrent. In order to determine the cellular interactions that are involved in gonadogenesis, we conducted a series of cell ablation experiments. Killing both of the progenitor germ cells, Z2 and Z3, does not have a significant effect on the somatic gonad. Despite the lack of germ cells, the 12-cell SPh forms

properly in J3-larvae. Adult animals have somatic gonads with two reflexed arms; however, these arms are quite small (Table 1A, row 1). As a result of their small size, germlineless gonadal arms are problematic to dissect for in vitro examination of tissues. In all animals examined by Nomarski microscopy in vivo, the gonadal arms turn dorsally and migrate very briefly back towards the center of the animal along the dorsal side. The germlineless gonadal arms are too short to meet at the center of the animal over the vulva and do not migrate back to the ventral side of the animal. The overall volume of the somatic tissues, sheath, spermatheca, and uterus, appears diminished. The failure of complete arm migration and the diminished size of the somatic tissues may be explained solely to the loss of volume resulting from the lack of a germ line. The resulting outward pressure from a mitotically reproducing and growing germ line may be an essential force for arm extension and for fully expanded somatic gonadal structures. Ablation of the entire germ line, Z2 and Z3, in *C. elegans* also results in small, reflexed gonadal arms (Kimble and White, 1981).

The altered geometry of the *P. pacificus* 4-cell primordium compared to *C. elegans* raises the possibility

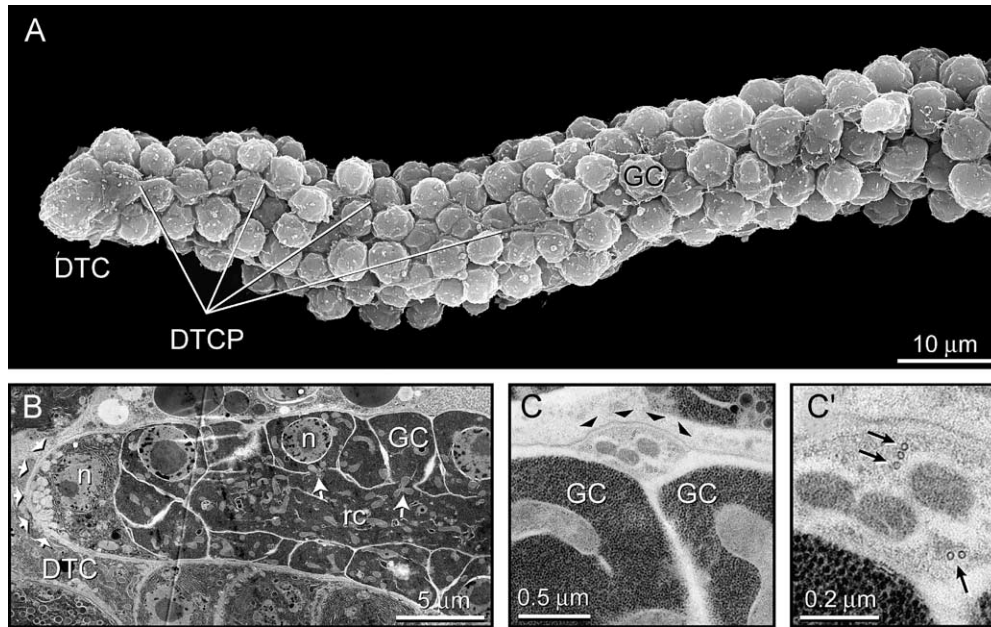


Fig. 5. The morphology of the *P. pacificus* adult hermaphrodite DTCs. (A) A scanning EM showing a DTC capping a dissected gonadal arm. The small irregular globes are individual germ cells. The DTC extends processes down the germ line. Germ cell, GC. Nucleus, n. Rachis, rc. DTC process, DTCP. (B) A TEM image showing a longitudinal section through the distal tip of a gonadal arm in an intact animal. Short white arrows mark the distal edge of the DTC. The distal cortex is highly vesiculated. The DTC and the rachis, or common cytoplasmic core of the germ line, are labeled; white arrows indicate openings between the rachis and individual germ cells. (C and C') A transverse section through a DTCP. The laminar side of the DTCP is marked by solid black triangles. Processes often hug the crevasse between adjacent germ cells. To the right is a blowup of the process. Black arrows mark microtubules.

that each germ cell precursor contributes solely to the single somatic arm generated by its associated somatic precursor partner. However, ablation of a single germ line precursor cell, either Z2 or Z3, in *P. pacificus* results in two normally sized gonadal arms in *P. pacificus*. The arms complete their extension appropriately and the somatic tissues are morphologically normal by Nomarski microscopy. However in many of these animals oocytes accumulate and stack in the gonadal arms (Table 1B, row 2), though the extent of stacking is not as striking as that seen in *C. elegans* homozygous for *fog* mutations, for feminization of the germ line (Barton and Kimble, 1990; Ellis and Kimble, 1994; Schedl and Kimble, 1988). Explanations for accumulation of oocytes include inefficient fertilization or reduced sperm number. In *C. elegans* animals that do not produce sperm, and thus fail to self-fertilize oocytes, fail to ovulate and oocytes stack in the arms of the gonad. To determine whether sperm quantity may be reduced or defective sperm may be present, brood counts from animals in which either Z2 or Z3 were ablated were performed. In these counts, ablated animals had brood sizes within the range of wild-type norms, suggesting that an appropriate amount of sperm is made and is functional (data not shown). Perhaps, the process of ovulation or fertilization is less efficient in these animals resulting in a production line bottleneck and thus the observed oocyte stacking. Future real-time video observation of these processes in ablated animals may yield insights into this phenotype. Likewise, in *C. elegans*, descendants of only Z2 or Z3 are sufficient to fill both gonadal arms, though no

oocyte stacking phenotype has been reported (Kimble and White, 1981).

Germ line development in P. pacificus requires the somatic gonad at multiple levels

The *P. pacificus* somatic gonad is required for proper regulation of the germ line. The somatic gonad is founded by Z1 and Z4 (Fig. 1B). In all ablated animals, loss of both Z1 and Z4 results in the absence of the vulva and the loss of all somatic gonadal structures. Without the somatic gonad, the progenitor germ cells Z2 and Z3 have variable developmental potential (Table 1C and D, rows 3–7). In some ablated animals, Z2 and Z3 arrest; in others, Z2 and Z3 proliferate and their progeny differentiate in an unregulated manner to produce germ cell conglomerates which can either remain in mitosis, enter into meiosis (i.e., pachytene), or differentiate as sperm. In no animals were only differentiated germ cells observed. In many conglomerates, mitotic plates could be observed indicating continuing proliferation. To quantify the size distribution of the tumors, we have divided them into three classifications, conglomerates with a few visible germ cells, that is, >2 but <50 cells, a “small tumor” if approximately 50–200 cells were present, and a “large tumor” if they contain >200 cells (Table 1C and D). In some animals, a large germ line tumor is produced that can contain many hundreds of germ cells at various stages of development, including mitosis, meiosis, and/or sperm. However, no oocytes are ever observed in Z1 and Z4 ablated animals. The penetrance of tumor formation

Table 1
Gonadal cell-ablation experiments in the *P. pacificus* hermaphrodite^a

Cell-ablation phenotype	Frequency ^b
<i>A. Ablation of both germ cell precursors, Z2 and Z3</i>	
1. Small empty somatic gonadal arms	38/38
<i>B. Ablation of a single germ cell precursor, either Z2 or Z3</i>	
2. Stacked oocytes in gonadal arms	16/27
<i>C. Ablation of the somatic gonad, Z1 and Z4 (strain PS312)^c</i>	
3. Small germ line tumor, sperm present (~50–200 cells)	4/35
4. A few germ cells visible (<50 cells)	2/35
<i>D. Ablation of the somatic gonad, Z1 and Z4 (strain PS1843)^c</i>	
5. Large germ line tumor (>200 cells)	4/22
6. Small germ line tumor (~50–200 cells)	7/22
7. A few germ cells visible (<50 cells)	7/22
<i>E. Ablation of both DTCs, Z1.aa and Z4.pp^c</i>	
8. Failure in both gonadal arms to extend	32/32
9. Glp phenotype (sperm count: ~37, N = 7 animals)	32/32
<i>F. Ablation of a single DTC, Z1.aa or Z4.pp</i>	
10. One armed gonad	21/21
<i>G. Ablation of both SS-precursor cells per arm^d</i>	
11. Sterile animals that do not lay any embryos	33/33
12. Animals with U-shaped bends	16/16
13. Germ lines with shortened mitotic and transition zones	17/19
14. Germ lines with extended pachytene zones	12/12
15. Germ lines lacking oocytes with diplotene chromosomes	23/23

^a Results reflect the effect of ablating the indicated cells on other gonadal tissues.

^b Given as a ratio of ablated animals with the given phenotype to total ablated animals assayed or as a ratio of dissected ablated gonadal arms with a given phenotype to total dissected ablated gonadal arms assayed. Animals assayed by dissection scope microscopy, Nomarski microscopy, and fluorescence microscopy.

^c All phenotypes observed in the same set of ablated animals.

^d Discrete phenotypes observed in different sets of ablated animals.

is highly dependent upon the genetic background of the *P. pacificus* strain used for the ablation experiment (Table 1C and D, compare rows 3 and 4 with rows 5 to 7). Ablated PS312 animals, the common laboratory strain, produced few and mostly small germ-line tumors (<100 cells). Ablated PS1843 animals, the mapping strain, had a high frequency of tumors and many larger tumors (>200 cells). This variability of phenotype argues strongly for a regulatory role for the somatic gonad on the germ line at all levels, that is, proliferation, meiosis, and the differentiation of gametes. Tissues of the somatic gonad are required to regulate many developmental processes. In particular, there are likely to be signals that inhibit unregulated mitosis and to initiate entry into meiosis. Also, as sperm may be present or absent in both small and large tumors, a signal to regulate the timing of spermatogenesis may also exist. Lastly, as oocytes are never seen, it seems likely that the somatic gonad is required to initiate oogenesis. In *C. elegans*, conglomerates of germ

cells have not been reported in hermaphrodite animals in which the somatic gonadal precursors, that is, Z1 and Z4 were ablated. Instead, in the absence of the somatic gonad the germ cell precursors arrest and die (Kimble and White, 1981). Therefore, in *P. pacificus* germ cells can survive, divide, and differentiate in the absence of the soma, while in *C. elegans* somatic tissues are required for germ cell survival.

The distal tip cells (DTCs)

A single distal tip cell caps the end of each *P. pacificus* ovotestis (Fig. 5A). TEM longitudinal sections show the DTCs of *P. pacificus* as crescents that cup the most distal cells in the mitotic region of the germ line (Fig. 5B). Also similar to *C. elegans* (Hall et al., 1999), scanning electron micrographs show that the DTCs extend very thin processes between the germ cells and the surrounding basement membrane (Fig. 5A, DTCP). Following individual processes in sequential transverse TEM sections of dissected gonadal arms, and along SEM images, indicates that individual processes can extend up to 17 cell diameters along the proximal–distal axis of the germ line. This would place the proximal terminus of the processes at the border of the mitotic region and the transition zone of the germ line. Unfortunately, it is impossible to assay both the processes and the state of the germ cell nuclei using EM and we are unable to observe the processes of the distal tip cell using in situ fluorescent stains. Thus, the precise extent of the processes with respect to the developmental zones of the germ line remains uncertain. Also, the processes in the fixed and sectioned samples may not completely reflect the full extent of the processes because fixation may result in contraction of the processes.

It is tempting to speculate that the distal tip cell in *P. pacificus* communicates with the underlying germ line. Consistent with this idea is that TEM micrographs through DTC processes in *P. pacificus* show the presence of microtubules that extend down the length of the process (Fig. 5C and C'). These microtubules may be used for the transport of signaling molecules. In *C. elegans*, a DTC also caps each gonadal arm and extends processes that can reach the approximate border of the transition zone. While many signaling molecules are known to be involved in crosstalk between the DTCs and the underlying germ cells in *C. elegans*, for example, members of the *Notch* pathway signal from the DTC to the germ line to maintain germ cells in a mitotic state (Kimble and Simpson, 1997), microtubules have yet to be reported in the DTC processes in *C. elegans*.

In *P. pacificus*, TEM micrographs through DTCs of adult animals and J3 larvae show that the leading edge of each DTC is highly vesiculated throughout the life of the animal (Fig. 5B). This large degree of vesiculation has not been observed in *C. elegans*. The exact role of this process, if any, in gonadogenesis is unknown. Each DTC leads the extension of one of the hermaphrodite gonadal arms. Again,

it is tempting to contemplate that the vesiculation may play a role in the extension of the gonadal arm in *P. pacificus*, perhaps by remodeling or establishing the basement membrane that surrounds the gonad during growth, or perhaps by influencing the membrane dynamics and migration of the DTC itself. A role for the DTC in remodeling the basement membrane has been suggested in *C. elegans* based upon morphology, cell-ablation studies, and genetic analysis of mutations in putative basement membrane remodeling proteases, for example, *gon-1* (Blelloch and Kimble, 1999; Blelloch et al., 1999).

The DTCs, Z1.aa and Z4.pp, are organizing centers in *P. pacificus*. Ablation of the DTCs in the late J2 stage shortly after their birth, the eight-cell stage, or in the early J3 stage, before formation of the SPH, results in a failure in arm extension. Ablation of both DTCs results in animals with no gonadal arms (Table 1E, row 8) and ablation of a single DTC results in animals with a one-armed gonad (Table 1F, row 10); the missing arm correlates with the arm in which the DTC was ablated. Additionally, no obvious mitotic or meiotic germ cells are present in *P. pacificus* adult hermaphrodites in which both DTCs were

ablated (Table 1, row 9). Nomarski microscopy and analysis of nuclei by DAPI staining show that only a few sperm are present in these animals. Thus, in the absence of the DTCs, the germ cells divide a few times and then differentiate as sperm. Ablation of the DTCs in a *C. elegans* hermaphrodite results in similar defects (Kimble and White, 1981). Thus, the two known organizing roles of the DTCs have been conserved between *P. pacificus* and *C. elegans*. Taken together with the results from ablating the somatic gonadal precursors, these experiments in *P. pacificus* suggest a complex regulation of germ line patterning by the somatic gonad throughout development.

The structure and development of the sheath

The sheath of *P. pacificus* has a novel morphology and represents the tissue that differs most strikingly between *P. pacificus* and *C. elegans* (Figs. 1, 6). In situ staining of dissected gonadal arms with DAPI and phalloidin, as well as tracings of serial transverse TEM sections through intact fixed *P. pacificus* adult hermaphrodite animals, indicate the

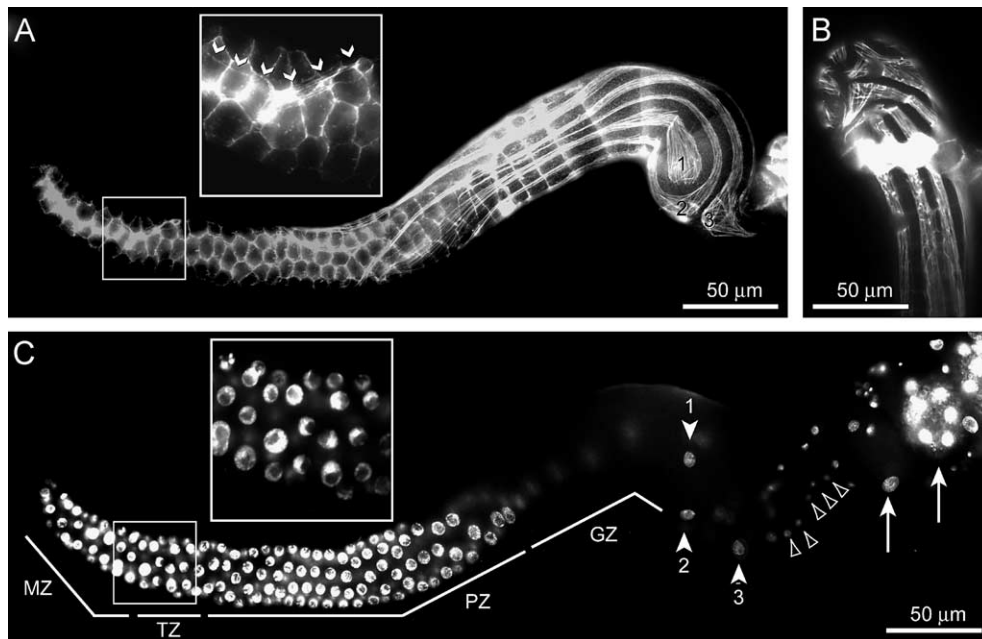


Fig. 6. The *P. pacificus* sheath has a novel morphology. A dorsal surface view of the same dissected gonadal arm is shown in panels A and C. This arm is the same arm shown in Fig. 4. Distal is to the left. (A and B) Phalloidin stains actin filaments in the sheath cells. Actin filaments align along the proximal–distal axis in the sheath cell processes. Phalloidin also stains the actin lining cell membranes. The hexagonal/pentagonal shapes in the distal germ line are the borders between germ cells. The proximal transverse lines are the borders between maturing oocytes. Spermathecal corridor cells also stain as they contain large amounts of cytoplasmic filamentous actin. (A) Individual sheath cells are numbered to correlate with the nuclei shown marked and labeled in panel C. Cell 1 is the central sheath cell of the gonad arm; Cell 2 is the U-shaped sheath cell of the gonad arm; Cell 3 is a lateral sheath cell; without a three dimensional reconstruction of the dissected gonad arm, it is not possible to determine if it is an outer or inner sheath cell (see Fig. 7). The insert is a blowup of the region indicated by the small box and correlates with the insert in panel C. The blowup shows the end of a sheath cell process. This process can be followed in sequential focal planes to connect to a sheath cell process on the lateral–ventral side of the gonad arm; V-shaped arrowheads mark the actin filaments of the process. (B) View of the back of the elbow-like joint in a dissected gonadal arm. The individual sheath cells interlock to form a tight cap on the germ line. The brightly staining corridor crosses over the underside of the distal gonadal arm. (C) Dapi staining reveals the morphology of nuclei. Germ line regions are indicated and labeled: Mitotic zone, MZ. Transition zone, TZ. Pachytene zone, PZ. Growth zone, GZ. The sheath cell nuclei are marked by arrowheads and numbered to correspond the labeled cells shown in panel A. Open tapered arrowheads mark the position of paired corridor cell nuclei. Arrows mark the position of embryos (see Fig. 4). The insert is a blowup of the region indicated by the small box and correlates with the insert in panel A. The blowup shows distal nuclei that are in mitosis, that is, round nuclei, and proximal nuclei in transition from mitosis to meiosis, that is, crescent-shaped nuclei.

P. pacificus sheath is composed of eight cells (Figs. 6–8). These cells are arranged in a roughly ring-like structure around the proximal most end of the germ line and extend long parallel processes distally along the germ line (Fig. 6A). As observed by double in situ staining of dissected adult gonadal arms with DAPI and phalloidin, individual processes can extend past the transition zone into the mitotic zone (Figs. 6A and C, compare inserts). While individual sheath processes and DTC processes undoubtedly overlap in this region, we have not been able to determine if the two types of processes actually make physical contact. This is largely due to our inability to observe both process types using the same technique. The

full extent of sheath cell processes is only observable in gently fixed and handled dissected gonad arms by in situ staining using phalloidin. More harsh in situ and SEM fixations and increased manipulation of the dissected gonad arms results in portions of the proximal sheath cell processes breaking off. Likewise, at present, DTC processes are observable only by EM. Based upon phalloidin in situ staining of dissected gonadal arms, SEM of dissected gonadal arms, and analysis of TEM serial sections through intact fixed worms, the sheath appears to fully encase only the most proximal two oocytes. Further distally, the sheath cell processes seem to be separated by gaps. In comparison, the *C. elegans* sheath is

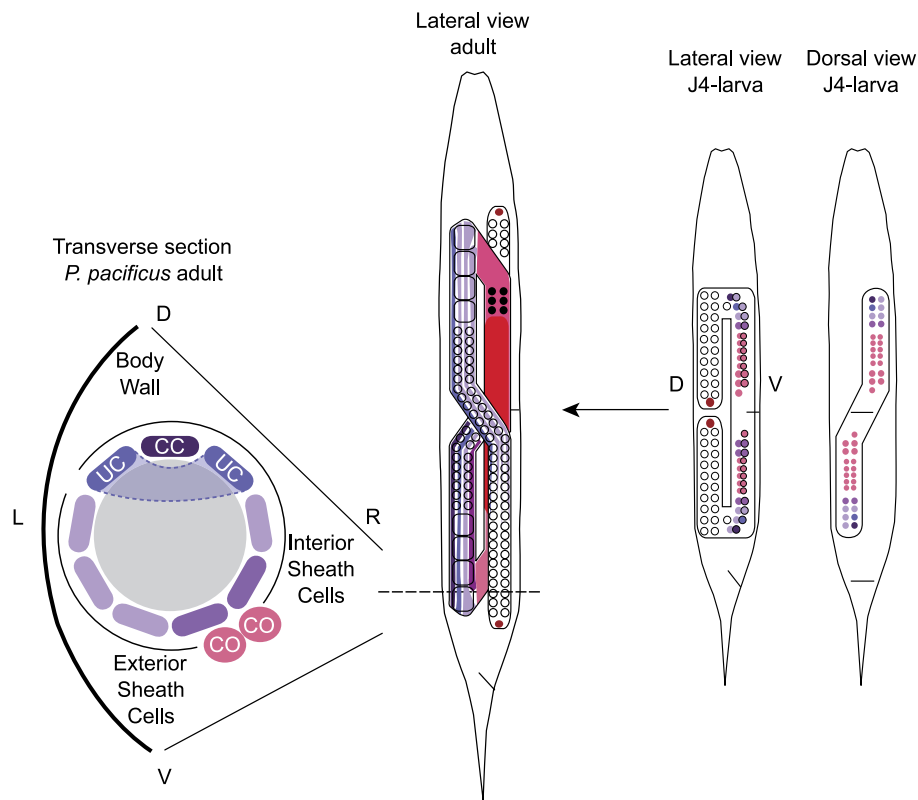


Fig. 7. Development of the *P. pacificus* sheath. General diagram description: Tissue types are coded as follows: Sheath, individual sheath cells and their associated processes are represented by discrete shades of purple. Spermatheca, pink. Uterus, red. DTC nuclei, dark red. Mitotic and meiotic germ cells, transparent circles. Oocyte, transparent rounded block. Sperm, solid black circle. Right diagram description: Two different views of a J4 stage larva are shown, a dorsal view and a lateral view. The nuclei of presumptive sheath and spermathecal cells are represented as solid colored circles. The nuclei of presumptive uterine cells are not shown. Germ cells are not shown in the dorsal view. In the early J4 stage, the distal somatic gonad cells form two aligned rows of cells that comprise the ventral portion of the gonadal arm, see dorsal view. The first four distal pairs of somatic cells become the sheath. They are the first somatic cells to show signs of differentiation, their nuclei enlarge slightly and eventually come to cap the proximal germ line, see lateral view. The four presumptive sheath cells facing the body wall of the animal are found within the same focal plane in a slightly curved line from the early J4 stage to the late J4 stage. The four cells of the interior row are also found in a single focal plane; however, in the mid J4-stage the two distal most presumptive sheath cells in this row break apart from the other two and change focal plane. In each gonadal arm, the former two cells assume a dorsal position overlying the germ line. Left diagram description: the left diagrams show a lateral view of an adult worm and a transverse cross-section through the elbow of an adult hermaphrodite gonadal arm. In the cross-section, sheath cell processes are shown as ovals and color-coded to match both their respective sheath cells shown in the adult diagram and the correlating presumptive sheath cells in the diagrams of the J4 stage larva. The two distal dorsal sheath cells assume unique disparate cell morphologies. The distal most cell, dark purple, develops a smooth round proximal edge and extends a single process distally down the germ line axis, we refer to this cell as the central cell, CC. Its partner cell, blue-violet, molds itself around the central cell and extends a process along either side of the central cell to form an extended U-shape. We refer to this cell as the U-cell, UC. It should be noted that this is the only cell that normally extends two processes. Each of the remaining sheath cells, that is, the four exterior cells and the remaining two interior cells, normally extend only a single process distally along the germ line. These remaining cells interlock at the posterior edge of the germ line to form a cap. The spermathecal corridor meets the sheath at a characteristic position between individual sheath cells, shown in medium purple, to form the elbow of the gonadal arm. The first pair of corridor cells, CO, is shown as a pair of pink circles in the transverse section.

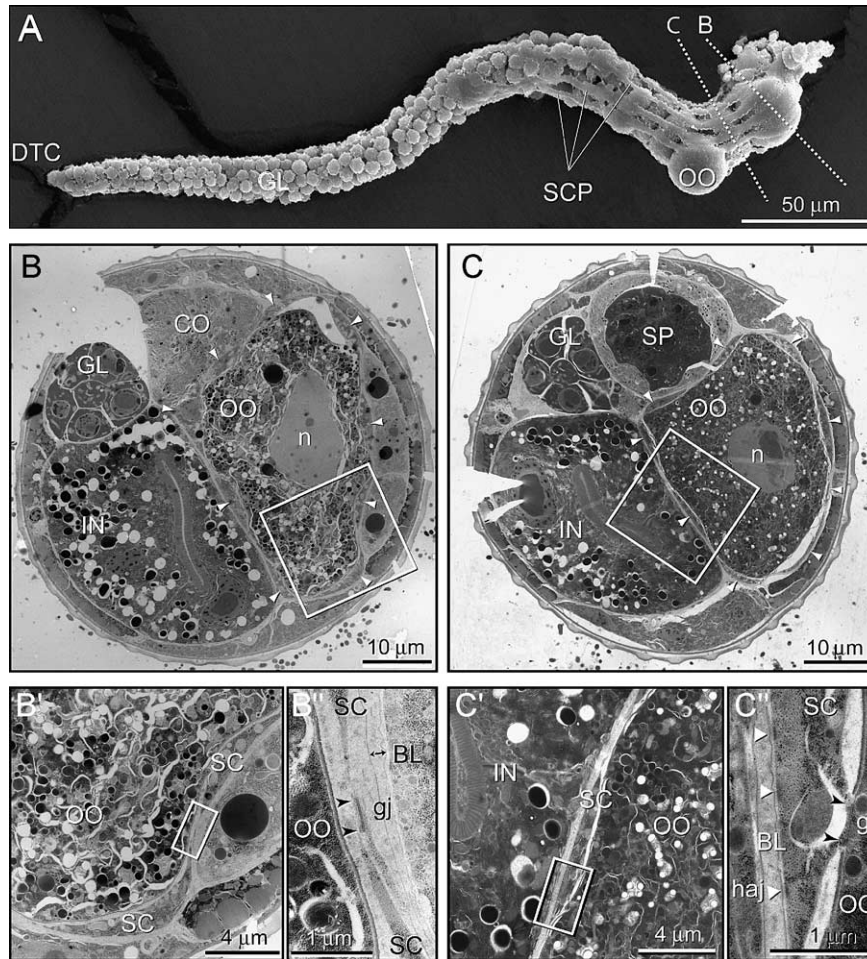


Fig. 8. Electron microscopy of the *P. pacificus* sheath. Micrographs are labeled as follows: Distal tip cell, DTC. Sheath cell process, SCP. Oocyte, OO. Germ line, GL. Intestine, IN. Nuclei, n. Sperm, SP. Spermathecal corridor cell, CO. Sheath cell, SC. Basal lamina, BL. Gap junction, gj. Hemi-adherens junction, haj. (A) A scanning EM of a dissected gonadal arm. Dashed lines represent the relative position along the proximal germ line of the transverse sections shown in panels B and C. (B and C) Transverse TEM sections through an intact adult hermaphrodite with sequential blowups. The frames in the larger micrographs represent the subsequent blowups. The largest blowups were taken from immediate neighboring sections. In the complete transverse sections, individual sheath cell processes are marked by long white triangles. Black arrowheads mark the extent of gap junctions. (B, B' and B'') The blowups show a gap junction between adjacent sheath cells. The width of the basal lamina surrounding the gonad is shown by double-headed arrow. (C, C' and C'') The blowups show the presence of a gap junction between a sheath cell and an oocyte. Contact between the sheath cell and the surrounding basal lamina is also demonstrated by the presence of hemi-adherens junctions, that is, electron dense dashes along the sheath cell membrane that are marked by white triangles.

composed of 10 cells that are organized in five pairs spaced along the most proximal portion of the germ line (Fig. 1) (Hall et al., 1999; Hird and White, 1993; Kimble and Hirsh, 1979; McCarter et al., 1997, 1999; Strome, 1986). Proximally, the first four pairs of adjacent sheath cells are interlocking and form a contiguous closed tube that extends around the bend and encases the proximal germ line. The most distal pair of sheath cells is positioned after the bend and does not fully encase the germ line, but leaves patches of exposed germ line, that is, in direct contact with the surrounding basement membrane (Fig. 1).

The *P. pacificus* sheath cell processes do not cross. When a less extended process is sandwiched by two larger more highly extended processes, it terminates when the outer processes move into closer proximity. When a sheath cell process takes a circumferential path, the path of adjacent processes also extends circumferentially along a parallel

pathway. These observations suggest that the extending sheath cell processes repulse and/or inhibit each other's extension and thus provide a potential mechanism for the regulation of sheath cell process extension along the proximal–distal axis.

The development of the sheath is highly regulated and reproducible in *P. pacificus*. Individual sheath cells have a characteristic position and morphology within the sheath (Figs. 6 and 7). Within a gonadal arm, the most distal sheath cell lies dorsally and has a round and smooth proximal edge and sends out a single process distally (Fig. 6A, cell 1). The cell immediately behind it forms a “U” shaped cell around the first cell by extending two processes distally, one on either side of the central cell (Fig. 6A, cell 2). This is the only cell that normally extends two processes. The remaining sheath cells extend a single process distally. The sheath cells interlock along the proximal end of the germ line to

form a cup that cradles the most proximal oocyte (Fig. 6B). The spermathecal corridor usually feeds into the sheath at a specified position between two predetermined sheath cells. Based both upon somatic nuclear position and morphology in dissected gonadal arms at different time points during the J4-stage and upon TEM reconstruction of adult gonadal arms using serial sections in intact adult hermaphrodites, we have constructed a model for the differentiation of the sheath (Fig. 7). Based upon this model, the presumptive sheath cell that will assume any given position in the adult tissue can putatively be distinguished prior to any signs of differentiation.

The sheath cells and the spermathecal corridor act as a ball and socket joint to form the elbow of the *P. pacificus* gonad bend. The cup formed by the sheath acts as the “socket” and the entrance to the spermathecal corridor meets the cup between two sheath cells at the ventral base of the germ line to provide the “ball”. This elbow forces the proximal germ line to the dorsal side of the animal (Fig. 1). Congruent with the striking difference in sheath structure in *C. elegans*, where no elbow is formed, the *C. elegans* germ line is free to continue unhindered around the bend directly into the spermathecal corridor and the spermatheca proper without an abrupt change in direction (Fig. 1) (Hall et al., 1999; Hirsh et al., 1976; Kimble and White, 1981). Thus, in *C. elegans*, due to differences in gonadal arm migration and in the morphology of somatic tissues, maturing oocytes are found continuously around the bend and along the ventral side of the animal.

In the *P. pacificus* SPH at the J3 stage, each arm has two precursor cells that give rise to only sheath and spermathecal tissues, the SS precursor cells (Felix et al., 1999). Ablation of both of the SS precursor cells results in defects in the gross morphology of the gonadal arms (Table 1G, row 12). These animals have large gonadal arms with a robust germ line; the basal lamina is sufficient to maintain the integrity of the reflexed gonadal arm. However, the characteristic elbow joint at the bend is missing. Instead the bend forms a smooth U-shaped turn reminiscent of that seen in *C. elegans*. Due to the lack of a physical constraint on the progress of the germ line in SS ablated *P. pacificus* animals, the germ line progresses evenly around the bend to the ventral side where it gets pushed into the uterus.

Concurrent with the difference in the gross morphology of the sheath, the sub-cellular structure of the sheath exhibits differences as well. The *P. pacificus* sheath is a contractile tissue. As such, the sheath cells contain many myofilament bundles, observed by phalloidin staining of actin, which likely aid in contraction (Figs. 6A and B). In the *P. pacificus* sheath cells, the myofilament bundles overwhelmingly align with the proximal–distal axis of the gonad and extend in parallel filaments down the length of the sheath cell processes (Fig. 6A). The *C. elegans* sheath is also a contractile tissue. In contrast to *P. pacificus*, however, the myofilament bundles within the sheath cells

are not aligned in a single direction. Also, different pairs of sheath cells along the proximal–distal axis show differential expression of myofilament bundles in *C. elegans*. In addition to the change in cytoskeletal elements, we have not observed yolk pores in *P. pacificus* sheath cells. In *C. elegans*, the sheath forms a continuous cover over the proximal germ line and large pore structures are required for the transport of yolk to the developing oocytes of the germ line (Hall et al., 1999; Kimble and Ward, 1988). These pore structures in *C. elegans* can easily be observed in TEM sections. Since the sheath of *P. pacificus* likely does not form a continuous tube around the developing proximal germ line, pores might not be required to transport yolk proteins through the sheath to nourish the germ line. Instead, yolk proteins may diffuse freely through the basement membrane and enter the *P. pacificus* germ line directly through the exposed gaps between sheath cell processes (Fig. 8A). Of course, failure to observe a structure is always suspect and a different method of observation or sample fixation may expose what has been previously undetectable.

Cell communication in the sheath

The sheath communicates with the germ line to regulate patterning. Novel patterning defects result from the ablation of both SS precursor cells in *P. pacificus* gonadal arms (Table 1G, rows 13 to 15). In SS precursor cell-ablated animals, the germ line is wild type in size, but the extent of the mitotic and meiotic zone changes. To observe the nuclear morphology of the germ line, dissected gonadal arms were stained with DAPI and phalloidin in developmentally staged gonad animals. To keep numbers directly comparable with the numbers given for wild type animals, gonads were observed in ablated staged animals that should have been able to lay eggs for approximately 24 h. The numbers given in parentheses represent sample averages based upon seven arms and their standard errors. In ablated animals, the mitotic zone and transition zone is smaller (12.28 ± 1.23 and 4 ± 0.58 , respectively) as determined by counting the number of nuclei in a line along the proximal–distal axis (Table 1G, row 13). More strikingly, the pachytene region is nearly twice as long, that is, 43 nuclei in length (42.86 ± 3.79) in comparison to 23 nuclei in a wild type germ line (Table 1G, row 14). The extended pachytene region has a variable nuclear morphology among ablated *P. pacificus* gonadal arms (Table 2). The extent of the growth zone remained constant (8.14 ± 0.72). It should be noted that in SS-ablated *P. pacificus* animals, the germ line is free to extend around the bend and push into the uterus, thus there is a larger linear region for the germ line to occupy. This alone does not explain the increase in the extent of the meiotic region. As the sizes of the growth zone and the mitotic and transition zones, either remain constant or are reduced, for example, this appears to be a specific “regulated”

Table 2

Nuclear morphology in the pachytene region of SS-ablated *P. pacificus* hermaphrodite animals

1. Mitotic appearing nuclei*
2. Mitotic divisions*
3. Pachytene nuclei, that is, condensed stranded DNA
4. Putative cell deaths
5. Large multi-lobed putatively polyploid nuclei*
6. Highly condensed DNA fragments*

Classification of nuclei and mitotic and meiotic stages are based upon the observation of nuclear morphology in DAPI stained ablated arms and by analogy to the morphology of wild type *P. pacificus* and *C. elegans* germ cells.

* Morphologies atypical for the wild type pachytene region.

expansion of the meiotic region. And as the mitotic zone, transition zone, and pachytene zone are putatively established prior to sheath or spermatheca differentiation (in particular sheath cell processes have not been extended), it seems likely that the sheath and spermatheca are not required to initiate patterning of these regions. Instead, it is more likely that they are required to maintain the extent of the zones and the smooth, sequential progression of germ cells through the different zones. In contrast to *P. pacificus*, ablation of both SS precursor cells per arm in *C. elegans* results in small gonadal arms (McCarter et al., 1997) that are morphologically similar to arms in which the germ line has been ablated. In these animals, germ cells fail to proliferate appropriately; mitotic cells enter meiosis prematurely and differentiate into sperm, that is, they exhibit a Glp phenotype (for germline proliferation) (Austin and Kimble, 1987; Kimble and White, 1981). However, ablation of a single SS precursor in *C. elegans* results in a large germ line with an extended pachytene region (McCarter et al., 1997). But, other than a failure to exit pachytene, no other defects are reported for this region in ablated *C. elegans* animals. Therefore, the *P. pacificus* sheath is only required for germ line patterning, while the *C. elegans* sheath is required for both germ line maintenance and patterning.

Ablation of both SS precursor cells in the *P. pacificus* gonad also results in novel defects in gametes. In SS-ablated animals, no oocytes have been observed in diakinesis with diplotene chromosomes (Table 1G, row 15). Many of these SS-ablated arms contain sperm as observed by Nomarski microscopy and by DAPI staining of dissected ablated arms. In contrast, oocytes in ablated *C. elegans* animals often have an Emo phenotype, that is, the DNA undergoes endomitotic replication in these oocytes without cell division; thus oocyte nuclei stain very brightly with DAPI. Additional defects include Fog phenotypes, that is, sperm are not present and oocytes stack up in the gonadal arm (McCarter et al., 1997).

Despite the presence of oocytes and sperm in many *P. pacificus* arms lacking sheath and spermatheca, embryos were never observed in these animals and neither eggs nor unfertilized oocytes were laid from ablated animals (Table

1G, row 11). The failure to produce embryos may be due to many reasons. First, as shown for *C. elegans* (McCarter et al., 1997, 1999), the sheath of *P. pacificus* is likely to have an active role in ovulation, thus, in the absence of sheath proper ovulation may not occur and this may not allow fertilization. Second, the state of the oocyte nuclei in ablated *P. pacificus* gonadal arms may result in defective or immature oocytes. Lastly, sperm may require the spermatheca and/or sheath for proper activation and/or differentiation, thus the sperm may be immature or defective. In support of the putative complex signaling among the sheath cells and between the sheath and the germ line, gap junctions can be found between sheath cells at their proximal ends (Fig. 8B) and between sheath cells and developing oocytes in the germ line (Fig. 8C) in TEM micrographs.

Three issues complicate any conclusions concerning the observed phenotypic differences between *P. pacificus* and *C. elegans* resulting from the ablation of the sheath spermathecal precursor cells. First, as previously stated, the germ line in SS-ablated animals is free to extend around the bend and push into the uterus. This allows the germ line to come into contact with putative molecular signals from the uterus, signals the germ line is normally protected from by the barrier formed by the sheath and spermathecal tissues. Second, when ablating the SS precursor cells in the *P. pacificus* SPh, the individual contributions of the sheath and the spermatheca to the resulting patterning defects cannot be determined unambiguously. However, the proximity of the sheath to the affected tissues and the gap junctions observed between the sheath and germ line makes it tempting to conclude that these patterning defects are due mostly to the absence of the sheath. Along these lines, genetic analysis and ablation of individual sheath cell precursors later during development in *C. elegans* indicates that the absence of the sheath alone is sufficient for many of the patterning defects described for the *C. elegans* germ line (McCarter et al., 1997). However, it should be kept in mind that patterning the gonad is complex and likely to involve multiple signals and cross talk between many tissues (Crittenden et al., 2003; Hansen et al., 2004a,b; Killian and Hubbard, 2004; Pepper et al., 2003). Likewise, a thorough investigation into the discrete roles of the sheath and spermathecae in *P. pacificus* will require a set of much more focused and detailed cell ablation experiments that are beyond the scope of this introduction to the hermaphrodite *P. pacificus* gonad. Third, some of the novel effects of ablating the sheath that we report here for *P. pacificus* may have been masked and inaccessible in the analogous experiments in *C. elegans*. It should be stressed, due to the Glp phenotype that results from a complete ablation, that many of the patterning defects in the *C. elegans* hermaphrodite germ line can only be observed in gonadal arms where a single SS precursor or a subset of the sheath cells were eliminated. Thus, the full effect of the loss of the sheath

upon later steps in germ line patterning cannot be assessed in *C. elegans*.

The spermatheca

The nematode spermatheca can be divided into two discrete sections, a corridor and the pouch-like spermatheca proper. The spermathecal corridor is composed of five pairs of cells (Figs. 4A and B) with an internal lumen through which mature oocytes, approximately 25 μm in width, must pass to enter the spermatheca proper. The lumen of the corridor is entirely absent when not expanded. These five pairs of cells appear to be specialized along the length of the corridor. The first two distal most pairs of corridor cells are larger, have a more blocky appearance, and do not stain as brightly as the subsequent three pairs when labeled with phalloidin to detect actin (Fig. 4B). The cytoplasm of these distal corridor cells is electron dense and rich in endoplasmic reticulum (ER) (Fig. 9A). The next three proximal pairs of corridor cells are slightly smaller, appear more rounded, and have a large amount of cytoplasmic actin in comparison to the first two pairs of corridor cells (Fig. 4B). The cytoplasm of the proximal three pairs of corridor cells contains much less ER and is less-electron dense and appears lighter in TEM sections (Fig. 9B). A light grey cloud of filamentous actin fills the cytoplasm facing the apical surface, that is, facing the lumen (Fig. 9B). The nuclei of all five pairs of corridor cells appear similar by DAPI staining. The corridor cells surround a proteinaceous-fluid filled passage through which mature oocytes are ovulated and enter the spermatheca and ultimately the uterus. TEM of sections through the corridor shows adherens-like junctions bound the apical surfaces between paired cells and between adjacent pairs of cells (Fig. 9C). In *C. elegans*, the tight corridor through which oocytes enter the spermatheca proper is composed of only four pairs of cells. Morphological distinctions along the corridor have not been reported in *C. elegans* (Hall et al., 1999; Kimble and Hirsh, 1979).

The *P. pacificus* spermatheca proper, or spermathecal pouch, is a morphologically distinct tissue composed of five cells that form a proteinaceous-fluid filled internal lumen for sperm storage. While the spermatheca proper is the storage site for the majority of the sperm (Fig. 9D), sperm can be found in the cup formed by the sheath and occasionally in the lumen of the corridor as well (Fig. 9C). The cells of the spermatheca proper are inter-locking pairs, adjacent pairs being transverse with respect to each other. A cross-section of the spermatheca at either the proximal or distal ends shows two spermathecal cells forming a hollow tube containing the sperm, each cell comprises an approximate semi circle. A cross-section in the center of the spermatheca proper shows four cells with each cell forming a quarter of the tube (Fig. 9D). Adjacent spermathecal cells are held together at their luminal surfaces by adherens-like junctions (Fig. 9F). The spermathecal lumen is held closed by stretches of putative septate-like junctions (data not shown). It seems likely that the septate-like junctions unzip to provide a larger lumen surface for the passage of eggs. The cytoplasm of spermathecal cells is histologically distinct from that of both spermathecal corridor cells and uterine cells (compare Figs. 9B and D, see Fig. 9E). A single cell of the spermatheca proper in *P. pacificus* shows a set of histological and morphological differences from the other four and may have a specialized function (data not shown). It covers a smaller portion of the spermathecal tube and appears to be thicker than the other five. This cell forms part of the junction with the uterus. In comparison, *C. elegans* spermathecal pouch cells exhibit a similar morphology to those in *P. pacificus*; they have analogous junctions with neighboring spermathecal pouch cells, and likely perform many of the same biological functions. However, the spermatheca proper of *C. elegans* is composed of 16 smaller cells (Kimble and Hirsh, 1979; McCarter et al., 1997).

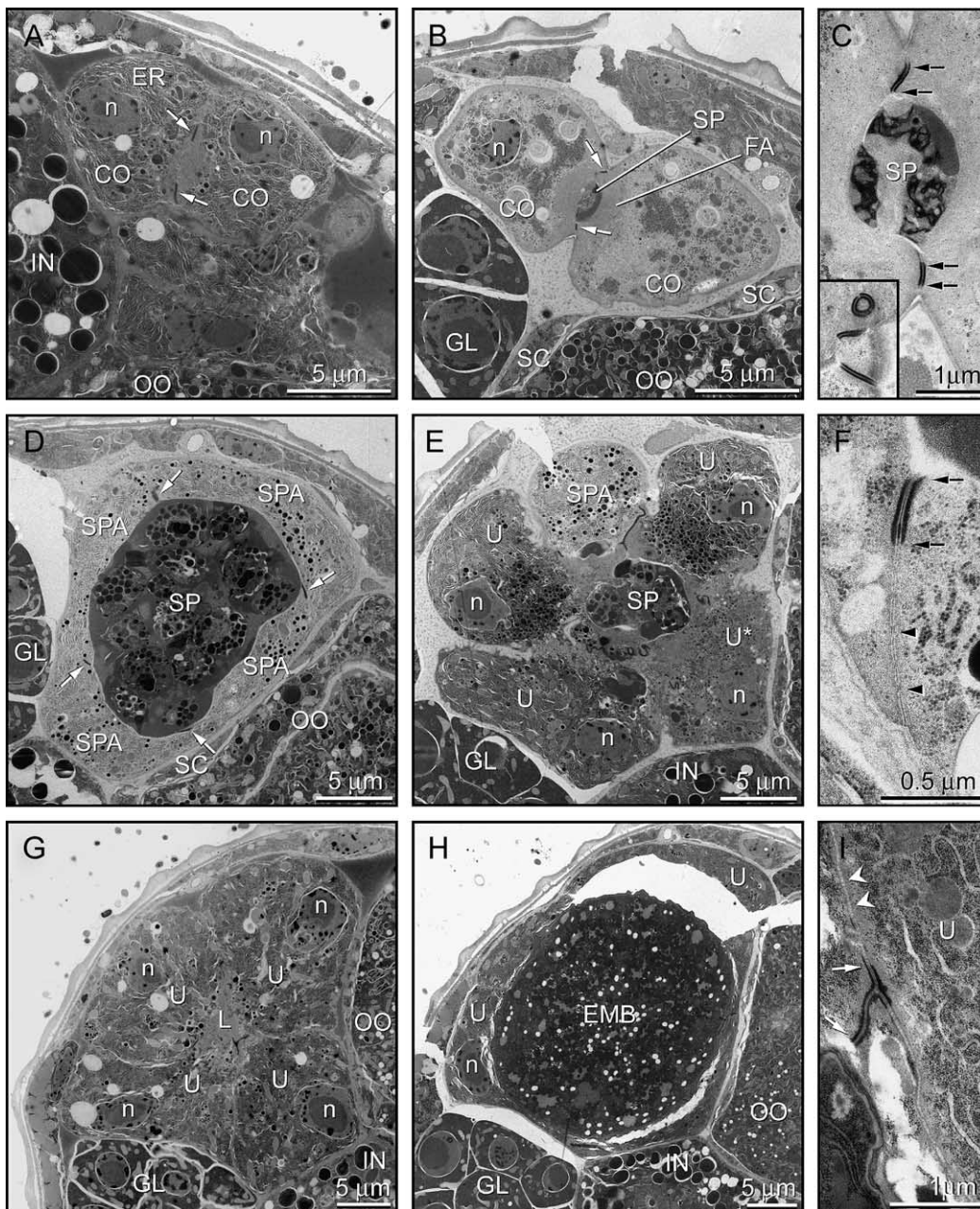
P. pacificus is missing a tissue in comparison to *C. elegans*. In *P. pacificus*, the spermathecal cells attach

Fig. 9. Electron microscopy of the *P. pacificus* spermatheca and uterus. Transverse TEM sections through the gonad. Micrographs are labeled as follows: Intestine, IN. Distal germ line, GL. Sheath cell, SC. Spermathecal corridor cell, CO. Spermatheca proper cell, SPA. Uterus cell, U. Oocyte, OO. Sperm, SP. Embryo, EMB. Endoplasmic reticulum, ER. Nucleus, n. Filamentous actin, FA. Lumen, L. Arrows indicate the position or extent of adherens-like junctions. Black triangles indicate gap junctions. White arrowheads indicate putative smooth/continuous septate-like junctions. Throughout the proximal gonad, the luminal surfaces of somatic cells are bounded by adherens-like junctions. Adherens junctions are conspicuous due to the presence of electron dense material along both membranes of adjacent cells. (A) Distal spermathecal corridor cells. The first two pairs of corridor cells are large and blocky in comparison to the last three pairs of corridor cells. Their cytoplasm is darker and they contain a large amount of ER in comparison to the more proximal corridor cells. (B) Proximal spermathecal corridor cells with a sperm. More proximal corridor cells have a lighter cytoplasm and contain less ER. Proximal corridor cells have a grey cloud of putative filamentous actin surrounding the lumen. This actin stains brightly with phalloidin. The lumen of the corridor is completely closed unless held open by an obstruction like the sperm cell shown. (C) Junctions between corridor cells. Adjacent pairs of corridor cells are tightly connected to each other. The surfaces of adjacent pairs of cells often form interlocking cytoplasmic fingers with each other that are held together with adherens-like junctions, see insert. (D) The spermatheca with sperm. Cells of the spermatheca proper contain many more electron dense vesicles in comparison with the proximal corridor cells and have less ER and a lighter, that is, less electron dense, cytoplasm than that of uterine cells. (E) The connection between the spermatheca and uterus. Uterine cells have a darker cytoplasm than spermathecal cells and contain a large amount of ER membrane. Few sperm are found outside the spermatheca in the uterus. Consistently in observed animals, a single uterine cell at the spermatheca/uterus junction, U*, and a single spermathecal cell, not shown, have distinct histological properties relative to their siblings. U* has less ER and fewer dark staining vesicles. (F) Junctions between cells of the spermatheca proper. Gap junctions and other junction types form between spermathecal cells on their lateral and laminar surfaces. (G) The empty uterus forms a cloverleaf like structure. The lumen of the uterus is almost entirely closed when embryos are not present. (H) The uterus with an embryo. The luminal surface of the uterus can expand greatly when an embryo is present. (I) Junctions between uterine cells. Putative smooth/continuous septate junctions and gap junctions, not shown, form between uterine cells on their lateral and laminar surfaces.

directly to the first cells of the uterus and entry from the spermatheca to the uterus is unrestricted. In contrast, in *C. elegans*, a multinucleated ring-shaped cell surrounds the junction between the spermatheca and uterus and creates a tight constriction between the two compartments. In *C. elegans*, these valve cells, one for each arm, contain a large amount of actin and strongly stain with phalloidin. In *P. pacificus*, neither Nomarski microscopy nor phalloidin staining for actin reveal valve cells similar to those of *C. elegans*. Similarly, valve cells are not seen in TEM micrographs of longitudinal sections through fixed intact *P. pacificus* adult hermaphrodites (Fig. 10). It seems likely, based on the difference in the turn of the gonad arm, the difference in sheath sub-cellular and gross morphological

structure, and the lack of valve cells, that ovulation in *P. pacificus* involves changes in the forces produced by the sheath and spermatheca, the direction of those forces, and the timing of events in comparison to *C. elegans*. Future real time video of ovulation is likely to clarify the process.

The *P. pacificus* spermatheca putatively provides an attractant for sperm. Despite the lack of a valve cell the sperm remain in the spermatheca in *P. pacificus* and when a sperm is pushed into the uterus by the passage of an egg it will migrate back into the spermatheca. Thus, like in *C. elegans*, there appears to be a signal that sperm can sense as a guidance cue to direct them. More detailed ablation studies to eliminate the spermatheca alone remain to be done in future investigations. Such ablations will clarify



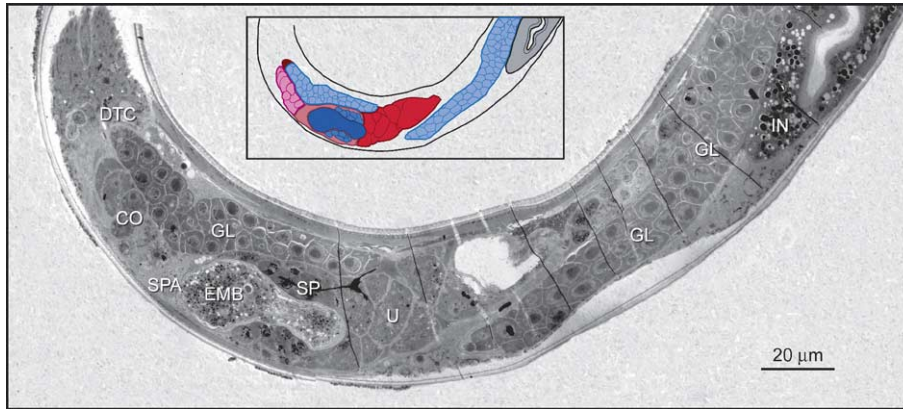


Fig. 10. A TEM longitudinal overview of the adult *P. pacificus* hermaphrodite gonad. Micrograph labeled as follows: Distal tip cell, DTC. Spermathecal corridor, CO. Spermatheca, SPA. Uterus, U. Germ line, GL. Sperm, SP. Embryo, EMB. Intestine, IN. Tissues are also color-coded in a cartoon: DTC, dark red. CO, pink. SPA, light red. U, bright red. GL, light blue. SP, medium blue. EMB, dark blue. IN, grey. The somatic gonadal tissues represent the proximal portion of one arm. The DTC and GL represent the distal portion of the other arm. Clearly, there are no valve cells to form a constriction between the spermatheca and uterus.

the roles of the spermatheca in interactions with other tissues, particularly interactions with sperm. It seems plausible that the spermatheca may be a central player in the interactions required for sperm activation and for the production of localization cues to direct the sperm to the point where they are needed for efficient fertilization of mature oocytes.

The uterus

Like the spermatheca, the uterus is also composed of interlocking cells. However, the uterus is morphologically distinct from the spermatheca. First, the uterus lacks a large population of congregating sperm cells. Second, the cytoplasm of the uterine cells is histologically different from that of spermathecal cells; it is darker (Fig. 9E). As in the spermatheca, one of the most distal uterine cells is histologically distinct from its siblings and is involved in forming the spermathecal-uterine junction (Fig. 9E). Similar to cells in the spermatheca, adjacent uterine cells are connected by adherens-like junctions on their apical edges (Fig. 9I). Additionally, various other types of junctions can be observed between adjacent uterine cells in the basal lateral membrane domains (Fig. 9I). Also, as in the spermatheca, the lumen of the uterus is tightly constricted in the absence of an embryo (compare Figs. 9G and H).

Ablations of the uterine precursor do not affect the rest of the gonad, but do affect vulval development (Sigrist and Sommer, 1999). In *P. pacificus*, one of the four ventral uterine precursor cells is destined to give rise to a special organizing cell, the anchor cell. This cell sends a signal to an underlying epidermal cell, P6.p, to form the center of the vulva (i.e., a primary vulval cell fate). As previously reported, ablation of the anchor cell after it is specified results in a failure of P6.p to adopt a normal primary fate (Sigrist and Sommer, 1999). Ablation of the two dorsal uterine precursors in *P. pacificus* at the SPh stage results in

only the absence of the tissues to which the ablated cells would give rise. No other obvious defects were observed for absence of the dorsal uterus in either the gonad or vulva. Ablations of uterus precursor cells in *C. elegans* affect the *C. elegans* gonad and vulva in an analogous manner (Kimble, 1981).

Conclusions

One goal of this analysis was to identify differences in the development and morphology of the hermaphrodite gonads of *P. pacificus* and *C. elegans*. We have found that there are differences at many levels (Table 3). First, the gross morphology of the *P. pacificus* hermaphrodite gonad is novel due to changes in many processes. Among these, the arms of the *P. pacificus* gonad migrate along a different path than those of *C. elegans* (Hedgecock et al., 1987; Kimble and White, 1981); relative to the length of the larval body, the arms turn dorsally at a more central position in *P. pacificus*. In *C. elegans*, a small group of heterochronic genes including *daf-9* and *daf-12* regulate the onset of the expression of the netrin receptor, UNC-5, in the DTC, which in turn is required for the dorsal migration (Gerisch et al., 2001; Mak and Ruvkun, 2004; Su et al., 2000). It may be speculated that heterochronic differences in the *P. pacificus* gonad may result in altered regulation of the expression of genes like *daf-9*, *daf-12*, and *unc-5* that shape the path of migration in *C. elegans*. This seems particularly plausible as *P. pacificus* shows many small differences in the timing of developmental events in comparison to the corresponding events in *C. elegans*. In addition to heterochronic changes, a new regulation or signal may have evolved in *P. pacificus* to initiate the ventral migration of the gonad later in development.

The gross morphology is also affected by changes in the composition and morphology of the individual tissues. We

Table 3

Differences between *P. pacificus* and *C. elegans**Morphological novelties*

1. The geometry of the 4-cell gonad
2. The path of arm migration
3. The shape of the bend
4. The number of oocytes in diakinesis
5. The size of sperm
6. The sub-cellular structure of the DTC
7. The gross morphology and cellular composition of the sheath
8. The subcellular structure of the sheath cells
9. The gross morphology and cellular composition of the spermatheca

Heterochronic differences

10. Timing of gamete differentiation with respect to life-stage
11. Timing of somatic gonad differentiation with respect to life-stage

Cell–cell signalling novelties

12. Effects of the somatic gonad, Z1 and Z4, on the germ line, Z2 and Z3
13. Effect of the sheath/spermatheca on the mitotic zone
14. Effect of the sheath/spermatheca on patterning in the pachytene zone
15. Effect of the sheath/spermatheca on gametogenesis

have shown that the number of cells that comprise the sheath and the spermatheca are different in *P. pacificus* in comparison to *C. elegans*. The *P. pacificus* sheath cells form a hand, that is, the cell bodies are at the very proximal end of the germ line and they extend processes down the germ line. Morphologically, this constrains the proximal germ line to the dorsal side of the animal and forces a very sharp elbow-like turn in the *P. pacificus* gonad instead of the smooth “U”-shaped turn known from *C. elegans*. As a final morphological novelty, there is no constriction between the spermatheca and the uterus in *P. pacificus* as the valve cells known from *C. elegans* are absent altogether.

There are still many unresolved issues ripe for future descriptive studies and cell manipulation analysis. First, it is obvious that a much more detailed series of ablation experiments will give new insights to the timing and roles of individual tissues and cells. Second, the gonad is a sexually dimorphic tissue and this study ignored the development of the male gonad in its entirety. Third, the phenotypic results from ablating the somatic gonad differ greatly between the strains of *P. pacificus* used. How does the intra-species variation compare to the inter-species variation in developmental processes?

Ultimately, the identification and comparison of developmental pathways involved in gonadogenesis in *P. pacificus* and *C. elegans* will demonstrate changes that have resulted in the novelties present in both species and the nematode gonad may serve as a paradigm for the study of evolution and development. A detailed analysis of cellular interactions should open the door to identifying candidate genes that have been studied in detail in either *P. pacificus* or *C. elegans* that are likely to have altered functions or regulation in the other nematode. For example, the arm migrations of *P. pacificus* already suggest a set of

heterochronic genes and cell surface proteins that may have altered regulatory cassettes. Both *P. pacificus* and *C. elegans* have diverged independently in significant ways from their last common ancestor. Only the ability to use forward genetics and reverse genetics coupled with phenotypic analysis in both organisms can begin to address the mechanisms by which changes have occurred. Forward genetics allows an unbiased identification of molecular players involved with specific developmental processes in both animals. Reverse genetics allows a quick study of homologous pathways when forward genetic studies and comparative morphology suggest the corresponding biological roles for a pathway differ between *P. pacificus* and *C. elegans*. With traditional genetics and detailed descriptive analysis combined with an integrated genomic map and knockdown techniques such as morpholinos and RNAi to impede gene function, the *P. pacificus* and *C. elegans* gonads together may prove to be a cornucopia for comparative biology.

Acknowledgments

We would like to thank Heinz Schwarz, Brigitte Sailer, and Jürgen Berger for technical assistance with TEM and SEM. We would like to thank Kellee Siegfried for insightful comments on the manuscript and the Sommer lab and the MPI for Entwicklungsbiologie for stimulating discussions concerning the work. We would also like to extend our appreciation to the anonymous reviewers for their helpful suggestions. D.R. was supported by a Human Frontiers in Science Grant for most of this work and by a Ruth L. Kirschstein National Research Service Award.

References

- Austin, J., Kimble, J., 1987. *gfp-1* is required in the germ line for regulation of the decision between mitosis and meiosis in *C. elegans*. *Cell* 51, 589–599.
- Baldwin, J.G., Frisse, L.M., Vida, J.T., Eddleman, C.D., Thomas, W.K., 1997. An evolutionary framework for the study of developmental evolution in a set of nematodes related to *Caenorhabditis elegans*. *Mol. Phylogenet. Evol.* 8, 249–259.
- Barton, M.K., Kimble, J., 1990. *fog-1*, a regulatory gene required for specification of spermatogenesis in the germ line of *Caenorhabditis elegans*. *Genetics* 125, 29–39.
- Blaxter, M., 1998. *Caenorhabditis elegans* is a nematode. *Science* 282, 2041–2046.
- Blaxter, M.L., De Ley, P., Garey, J.R., Liu, L.X., Scheldeman, P., Vierstraete, A., Vanfleteren, J.R., Mackey, L.Y., Dorris, M., Frisse, L.M., Vida, J.T., Thomas, W.K., 1998. A molecular evolutionary framework for the phylum Nematoda. *Nature* 392, 71–75.
- Blelloch, R., Kimble, J., 1999. Control of organ shape by a secreted metalloprotease in the nematode *Caenorhabditis elegans*. *Nature* 399, 586–590.
- Blelloch, R., Anna-Arriola, S.S., Gao, D., Li, Y., Hodgkin, J., Kimble, J., 1999. The *gon-1* gene is required for gonadal morphogenesis in *Caenorhabditis elegans*. *Dev. Biol.* 216, 382–393.

- Brenner, S., 1974. The genetics of *Caenorhabditis elegans*. *Genetics* 125, 29–39.
- Crittenden, S.L., Troemel, E.R., Evans, T.C., Kimble, J., 1994. GLP-1 is localized to the mitotic region of the *C. elegans* germ line. *Development* 120, 2901–2911.
- Crittenden, S.L., Eckmann, C.R., Wang, L., Bernstein, D.S., Wickens, M., Kimble, J., 2003. Regulation of the mitosis/meiosis decision in the *Caenorhabditis elegans* germline. *Philos. Trans. R. Soc. Lond., Ser. B Biol. Sci.* 358, 1359–1362.
- Ellis, R.E., Kimble, J., 1994. Control of germ cell differentiation in *Caenorhabditis elegans*. *Ciba Found. Symp.* 182, 179–188 (discussion 189–192).
- Epstein, H.F., Shakes, D.C., 1995. *Caenorhabditis elegans*: Modern Biological Analysis of an Organism. Academic Press, San Diego.
- Felix, M.A., Hill, R.J., Schwarz, H., Sternberg, P.W., Sudhaus, W., Sommer, R.J., 1999. *Pristionchus pacificus*, a nematode with only three juvenile stages, displays major heterochronic changes relative to *Caenorhabditis elegans*. *Proc. R. Soc. Lond., Ser. B Biol. Sci.* 266, 1617–1621.
- Gerisch, B., Weitzel, C., Kober-Eisermann, C., Rottiers, V., Antebi, A., 2001. A hormonal signaling pathway influencing *C. elegans* metabolism, reproductive development, and life span. *Dev. Cell* 1, 841–851.
- Gould, S.J., 1977. *Ontogeny and Phylogeny*. The Belknap Press of Harvard University, Cambridge, MA.
- Hall, D.H., Winfrey, V.P., Blauer, G., Hoffman, L.H., Furuta, T., Rose, K.L., Hobert, O., Greenstein, D., 1999. Ultrastructural features of the adult hermaphrodite gonad of *Caenorhabditis elegans*: relations between the germ line and soma. *Dev. Biol.* 212, 101–123.
- Hansen, D., Hubbard, E.J., Schedl, T., 2004a. Multi-pathway control of the proliferation versus meiotic development decision in the *Caenorhabditis elegans* germline. *Dev. Biol.* 268, 342–357.
- Hansen, D., Wilson-Berry, L., Dang, T., Schedl, T., 2004b. Control of the proliferation versus meiotic development decision in the *C. elegans* germline through regulation of GLD-1 protein accumulation. *Development* 131, 93–104.
- Hausen, P., Riebesell, M., 2002. A simple flow-through micro-chamber for handling fragile, small tissue explants and single non-adherent cells. *Methods Cell Sci.* 24, 165–168.
- Hedgecock, E.M., Culotti, J.G., Hall, D.H., Stern, B.D., 1987. Genetics of cell and axon migrations in *Caenorhabditis elegans*. *Development* 100, 365–3682.
- Hird, S.N., White, J.G., 1993. Cortical and cytoplasmic flow polarity in early embryonic cells of *Caenorhabditis elegans*. *J. Cell Biol.* 121, 1343–1355.
- Hirsh, D., Oppenheim, D., Klass, M., 1976. Development of the reproductive system of *Caenorhabditis elegans*. *Dev. Biol.* 49, 200–219.
- Hohenberg, H., Mannweiler, K., Muller, M., 1994. High-pressure freezing of cell suspensions in cellulose capillary tubes. *J. Microsc.* 175 (Pt. 1), 34–43.
- Hubbard, E.J., Greenstein, D., 2000. The *Caenorhabditis elegans* gonad: a test tube for cell and developmental biology. *Dev. Dyn.* 218, 2–22.
- Jungblut, B., Sommer, R.J., 2000. Novel cell–cell interactions during vulva development in *Pristionchus pacificus*. *Development* 127, 3295–3303.
- Kadyk, L.C., Kimble, J., 1998. Genetic regulation of entry into meiosis in *Caenorhabditis elegans*. *Development* 125, 1803–1813.
- Killian, D.J., Hubbard, E.J., 2004. *C. elegans* pro-1 activity is required for soma/germline interactions that influence proliferation and differentiation in the germ line. *Development* 131, 1267–1278.
- Kimble, J., 1981. Alterations in cell lineage following laser ablation of cells in the somatic gonad of *Caenorhabditis elegans*. *Dev. Biol.* 87, 286–300.
- Kimble, J., Hirsh, D., 1979. The postembryonic cell lineages of the hermaphrodite and male gonads in *Caenorhabditis elegans*. *Dev. Biol.* 70, 396–417.
- Kimble, J., Simpson, P., 1997. The LIN-12/Notch signaling pathway and its regulation. *Annu. Rev. Cell Dev. Biol.* 13, 333–361.
- Kimble, J., Ward, S., 1988. Germ-line development and fertilization. In: Wood, W.B. (Ed.), *The Nematode Caenorhabditis elegans*. Cold Spring Harbor Laboratory Press, Plainview, NY, pp. 191–213.
- Kimble, J.E., White, J.G., 1981. On the control of germ cell development in *Caenorhabditis elegans*. *Dev. Biol.* 81, 208–219.
- Mak, H.Y., Ruvkun, G., 2004. Intercellular signaling of reproductive development by the *C. elegans* DAF-9 cytochrome P450. *Development* 131, 1777–1786.
- Mathies, L.D., Henderson, S.T., Kimble, J., 2003. The *C. elegans* Hand gene controls embryogenesis and early gonadogenesis. *Development* 130, 2881–2892.
- McCarter, J., Bartlett, B., Dang, T., Schedl, T., 1997. Soma-germ cell interactions in *Caenorhabditis elegans*: multiple events of hermaphrodite germline development require the somatic sheath and spermathecal lineages. *Dev. Biol.* 181, 121–143.
- McCarter, J., Bartlett, B., Dang, T., Schedl, T., 1999. On the control of oocyte meiotic maturation and ovulation in *Caenorhabditis elegans*. *Dev. Biol.* 205, 111–128.
- McKinney, M.L., 1988. Heterochrony in Evolution: A Multidisciplinary Approach. In: Stehli, F.G., Jones, D.S. (Eds.), *Top. Geobiol.*, vol. 7. Plenum, New York, pp. 348.
- Pepper, A.S., Lo, T.W., Killian, D.J., Hall, D.H., Hubbard, E.J., 2003. The establishment of *Caenorhabditis elegans* germline pattern is controlled by overlapping proximal and distal somatic gonad signals. *Dev. Biol.* 259, 336–350.
- Pires-daSilva, A., Sommer, R.J., 2003. The evolution of signalling pathways in animal development. *Nat. Rev., Genet.* 4, 39–49.
- Pires-daSilva, A., Sommer, R.J., 2004. Conservation of the global sex determination gene *tra-1* in distantly related nematodes. *Genes Dev.* 18, 1198–1208.
- Rudel, D., Sommer, R.J., 2003. The evolution of developmental mechanisms. *Dev. Biol.* 264, 15–37.
- Schedl, T., Kimble, J., 1988. *fog-2*, a germ-line-specific sex determination gene required for hermaphrodite spermatogenesis in *Caenorhabditis elegans*. *Genetics* 119, 43–61.
- Siegfried, K.R., Kimble, J., 2002. POP-1 controls axis formation during early gonadogenesis in *C. elegans*. *Development* 129, 443–453.
- Siegfried, K.R., Kidd III, A.R., Chesney, M.A., Kimble, J., 2004. The *sys-1* and *sys-3* genes cooperate with Wnt signaling to establish the proximal–distal axis of the *Caenorhabditis elegans* gonad. *Genetics* 166, 171–186.
- Sigrist, C.B., Sommer, R.J., 1999. Vulva formation in *Pristionchus pacificus* relies on continuous gonadal induction. *Dev. Genes Evol.* 209, 451–459.
- Simpson, P., 2002. Evolution of development in closely related species of flies and worms. *Nat. Rev., Genet.* 3, 907–917.
- Sommer, R.J., 1997. Evolutionary changes of developmental mechanisms in the absence of cell lineage alterations during vulva formation in the *Diplogastridae* (Nematoda). *Development* 124, 243–251.
- Sommer, R.J., 2000. Evolution of nematode development. *Curr. Opin. Genet. Dev.* 10, 443–448.
- Sommer, R.J., 2001. As good as they get: cells in nematode vulva development and evolution. *Curr. Opin. Cell Biol.* 13, 715–720.
- Sommer, R.J., Sternberg, P.W., 1996a. Apoptosis and change of competence limit the size of the vulva equivalence group in *Pristionchus pacificus*: a genetic analysis. *Curr. Biol.* 6, 52–59.
- Sommer, R.J., Sternberg, P.W., 1996b. Evolution of nematode vulval fate patterning. *Dev. Biol.* 173, 396–407.
- Sommer, R.J., Carta, L.K., Kim, S.Y., Sternberg, P.W., 1996. Morphological, genetic and molecular description of *Pristionchus pacificus* sp.n. (Nematoda: Neodiplogastridae). *Fundam. Appl. Nematol.* 19, 511–521.
- Srinivasan, J., Pires-daSilva, A., Gutierrez, A., Zheng, M., Jungblut, B., Witte, H., Schlak, I., Sommer, R.J., 2001. Microevolutionary analysis of

- the nematode genus *Pristionchus* suggests a recent evolution of redundant developmental mechanisms during vulva formation. *Evol. Dev.* 3, 229–240.
- Strome, S., 1986. Fluorescence visualization of the distribution of microfilaments in gonads and early embryos of the nematode *Caenorhabditis elegans*. *J. Cell Biol.* 103, 2241–2252.
- Su, M., Merz, D.C., Killeen, M.T., Zhou, Y., Zheng, H., Kramer, J.M., Hedgecock, E.M., Culotti, J.G., 2000. Regulation of the UNC-5 netrin receptor initiates the first reorientation of migrating distal tip cells in *Caenorhabditis elegans*. *Development* 127, 585–594.
- Sudhaus, W., Fitch, D., 2001. Comparative studies on the phylogeny and systematics of the Rhabditidae (Nematoda). *J. Nematol.* 33, 1–70.
- Sudhaus, W., Fürst von Lieven, A., 2003. A phylogenetic classification and catalogue of the *Diplogastridae* (Secernentea). *J. Nematode Morphol. Syst.* 6, 43–90.